



## Paleoenvironmental significance of growth story of long-living deep-water acervulinid macrooids from Kikai-jima shelf, Central Ryukyu Islands, Japan

Davide Bassi <sup>a,\*</sup>, Juan Carlos Braga <sup>b</sup>, Ryuji Asami <sup>c</sup>, Kazuhisa Goto <sup>d</sup>, Sönke Szidat <sup>e</sup>, Hideko Takayanagi <sup>c,f</sup>, Yasufumi Iryu <sup>c,f</sup>

<sup>a</sup> Dipartimento di Fisica e Scienze della Terra, Università degli Studi di Ferrara, via Saragat 1, 44122 Ferrara, Italy

<sup>b</sup> Departamento de Estratigrafía y Paleontología, Universidad de Granada, Campus Fuentenueva s/n, 18002 Granada, Spain

<sup>c</sup> Institute of Geology and Paleontology, Graduate School of Science, Tohoku University, Aobayama, Sendai 980-8578, Japan

<sup>d</sup> Department of Earth and Planetary Science, The University of Tokyo, 7-3-1, Hongo, Bunkyo-ku, Tokyo 113-0033, Japan

<sup>e</sup> Department of Chemistry, Biochemistry and Pharmaceutical Sciences & Oeschger Centre for Climate Change Research, University of Bern, Freiestrasse 3, 3012 Bern, Switzerland

<sup>f</sup> Advanced Institute for Marine Ecosystem Change (WPI-AIMEC), Tohoku University, Sendai 980-8578, Japan

### ARTICLE INFO

Editor: M Elliot

#### Keywords:

*Acervulina*  
Biogenic nodules  
Bioerosions  
Mesophotic setting  
Holocene  
Ryukyu Islands

### ABSTRACT

Macrooids are unattached centimetre-sized nodules built by encrusting invertebrates. Encrusting foraminifera (*Acervulina inhaerens*) and subordinate thin coralline algae form extensive macroid beds on sandy and gravelly bioclastic carbonates off Kikai-jima, on a coral-reef-related island shelf, in the Central Ryukyu Islands, Japan. At water depths from 75 to 100 m, the beds consist of spheroidal and sub-spheroidal macroids, c. 6 cm in mean diameter, with asymmetric concentric inner arrangement. The macroids are bioeroded by *Entobia*, *Maeandropolydora*, *Trypanites*, *Gastrochaenolites*, and microborings. They generally show two distinct growth stages separated by an abraded rugged surface deeply colonized by borers, mainly *Entobia*. Radiocarbon dating yielded an oldest age of c. 4400 cal yr BP for the earliest acervulinid growth, whereas the second stages were much younger, ranging in age from c. 1500 cal yr BP to present day. Datings of the two growth stages in five specimens indicate that active growth and growth interruption were not synchronous in the different nodules. For c. 4400 years the macroids grew within an estimated maximum range of palaeotemperature changes of c. 4.7 °C, under chronic oligotrophic to mesotrophic conditions, low-level hydrodynamism and low sedimentation rates. The lack of synchronicity among individual macroids rules out catastrophic events and ecosystem-wide environmental changes as possible causes of growth interruption. Random biogenic mobilization and temporal occupation of the macroid surface by organisms with no rigid skeleton and/or biofilms likely interrupted acervulinid growth at individual macroid scale. The environmental conditions in which Kikai-jima macroid beds develop do not support interpretations of acervulinid macroid accumulations during Paleocene–Eocene Thermal Maximum (PETM) and Middle Eocene Climatic Optimum (MECO) events in the Western Tethys as indicators of eutrophic conditions.

### 1. Introduction

Biogenically coated grains consist of a nucleus and successive growths of encrusting organisms. Coralline red algae and encrusting acervulinid foraminifera build free-living, centimetre-sized nodules, called rhodoliths and macrooids, depending on the relative abundance of the building organisms (e.g., Hottinger, 1983; Prager and Ginsburg, 1989; Foster et al., 2013). These nodules create important marine habitats over loose sedimentary substrates supporting highly diverse and

often unique biological communities, the so-called rhodolith or macrooid beds (e.g., Amado-Filho et al., 2017; Veras et al., 2020), which occur from very shallow-water settings to the base of the photic zone (e.g., Reiss and Hottinger, 1984; Iryu et al., 1995; Kamenos et al., 2017; Bracchi et al., 2023; Caron et al., 2023).

Coralline algae and encrusting foraminifera occur with varying relative abundances in repetitive or randomly arranged superimposed growth stages. Occasional or frequent overturning of biogenic nodules, generally achieved by currents and/or biological activity, is likely to be

\* Corresponding author.

E-mail address: [bsd@unife.it](mailto:bsd@unife.it) (D. Bassi).

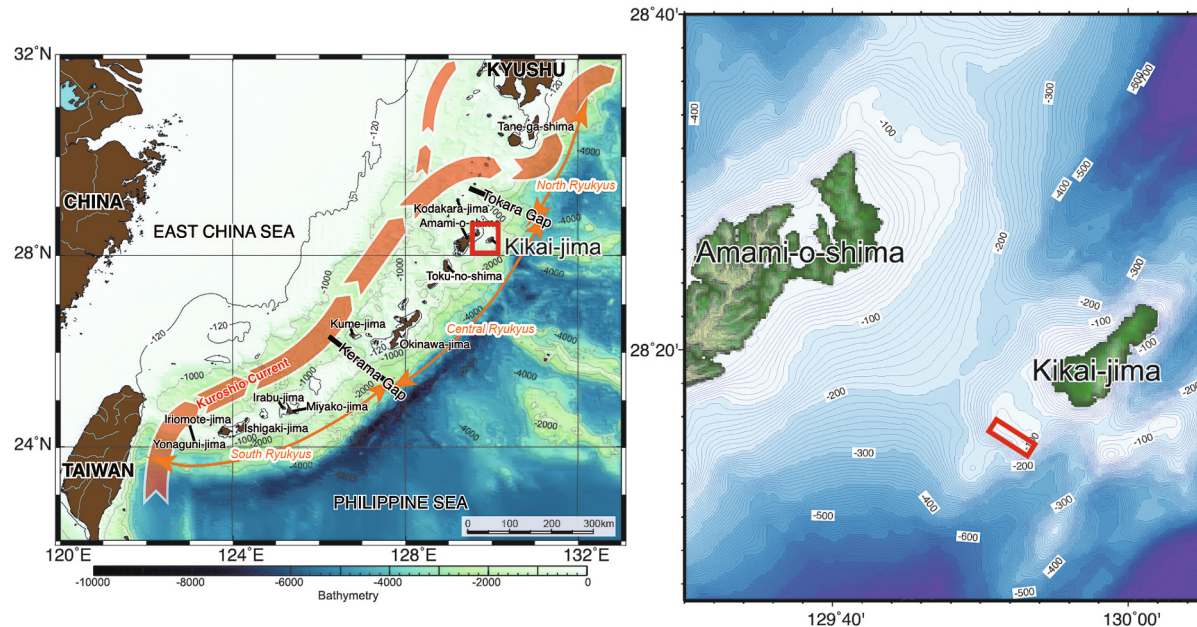


**Fig. 1.** Geographical location of the dredged area. This area is an island shelf off south-west Kikai-jima, Central Ryukyu Islands, Japan.

a prerequisite for nodule accretion (e.g., Hottinger, 1983; Prager and Ginsburg, 1989; Aguirre et al., 2017). The different shapes and internal structures of these nodules record changes in environmental factors, such as hydrodynamic conditions, substrate characteristics, trophic levels and sedimentation rate (e.g., Adey and Macintyre, 1973; Prager and Ginsburg, 1989; Foster et al., 2013; Aguirre et al., 2017; Sletten et al., 2017; Brasileiro et al., 2018; Támega et al., 2019; O'Connell et al., 2021; Bracchi et al., 2023). It has been assumed that changes in these environmental factors produce similar effects in rhodolith and macrooids with different proportions of coralline algae and encrusting foraminifera (e.g., Prager and Ginsburg, 1989; Aguirre et al., 1993; Baarli et al., 2012). These nodules are made of calcitic skeletons with high preservation potential as fossils and they form meter-thick fossil accumulations in many cases throughout the Late Cretaceous to the Cenozoic. As recorders of environmental changes for long time spans, they are useful tools for palaeoenvironmental reconstructions (e.g., Bassi et al., 2010; Johnson et al., 2011; Aguirre et al., 2012, 2017).

Abrupt transitions in age have been noted from older bored and infilled cores to the still-living outer layers, indicating major discontinuities in growth (e.g., McMaster and Conover, 1966; Focke and Geblein, 1978; Bosence and Pedley, 1982; Prager and Ginsburg, 1989; Littler et al., 1991; Halfar et al., 2013; Brasileiro et al., 2018; Vale et al., 2018; Lewis et al., 2017). These abrupt transitions in age have been interpreted as due to the intermittent growth of rhodolith beds, interrupted by changes in water energy and sedimentation rate (Littler et al., 1991; Matsuda and Iryu, 2011; Figueiredo et al., 2015; Vale et al., 2022). The longevity of the rhodolith beds has been discussed for paleoenvironmental and paleoclimate analyses (Adey and Macintyre, 1973; Frantz et al., 2000; van der Heijden and Kamenos, 2015; Aguirre et al., 2017). It has been assumed so far that individual rhodoliths in a single bed have similar growth stories, although their morphologies can greatly vary. In the fossil record, several study cases described and interpreted multi-story rhodoliths (e.g., Checconi et al., 2010; Murru et al., 2015; Aguirre et al., 2017; Bassi et al., 2017; Aguirre and Braga, 2022) and macrooids (e.g., Caratelli et al., 2021; Brandano and Tomassetti, 2022) pointing out that temporary burial is a common phenomenon in rhodolith and macrooid beds.

Rhodolith and macroid deposits have been extensively described in fossil and modern deposits from the Ryukyu Islands. Pleistocene Ryukyu reef-complex limestones are characterized by extensive rhodolith

deposits which formed in deep fore-reef to shelf settings (Nakamori et al., 1995; Iryu et al., 1998; Sagawa et al., 2001). There are numerous reports of modern rhodolith and macroid analogues from a variety of Ryukyu areas, ranging from 50 to 170 m water depth (Iryu, 1984, 1985; Iryu et al., 1995; Matsuda and Iryu, 2011; Bassi et al., 2012, 2020). These Ryukyu areas represent mesophotic ecosystems located at lower mesophotic depths (>60 m; Sinniger et al., 2019). The oldest dated foraminiferal-algal nodules known so far in Ryukyu macroid beds have been reported from Tarama-jima and Okinawa jima, giving ages of  $6465 \pm 45$  BP at 166 m water depth (Tsuji, 1993) and  $2750 \pm 70$  BP at 66 m water depth (Matsuda and Nohara, 1994; Matsuda and Iryu, 2011), respectively.

Information about ecological processes in acervulinid macroids and data regarding the temporal window of their development are scarce. Consequently, there needs to be more consensus about what ecological changes are recorded in macroids during the acervulinid growth and, in turn, which are the main ecological constraints to their growth.

This study assesses the environmental controls that affected living deep-water macrooids sampled at the mesophotic 75–100 m water depth off Kikai-jima, on a coral-reef-related island shelf in the Central Ryukyu Islands (Japan). We examine whether these deep-water macrooids show growth stages by their inner arrangement and bioerosion and estimate the growth-stage durations by radiocarbon dating. We also investigate the possible mechanisms that brought about interruptions in their growth.

## 2. Geographical setting

The Ryukyu Islands represent an active arc formed by subduction of the Philippine Sea Plate beneath the Eurasia Plate. The islands are made up of different rock types ranging in age from the Mesozoic to the Pleistocene (Ujié and Nishimura, 1992). The extensively developed Pleistocene carbonate and mixed siliciclastic-carbonate terraces reach up to c. 200 m in altitude (Nakamori et al., 1995; Watanabe et al., 2023).

Coral reefs rim most Ryukyu islands with a reef slope reaching water depths of >50 m (Hori, 1983). The area, from which the macrooids have been sampled, located off southwest Kikai-jima, is an island shelf with water depths from c. 60 to 110 m (Fig. 1). The seafloor in the Kikai-jima shelf at these water depths is characterized by an undulating and irregular topography with mobile sandy and gravelly bioclastic

**Table 1**

Analytical data for radiocarbon calibrated ages of the studied macroids. See Fig. 1 for sample geographic locations and Figs. 4–6 for location of the dated spots in the studied macroids.

Specimen	Sample code	Lab codes	Conventional $^{14}\text{C}$ age (years BP)				Calibrated $^{14}\text{C}$ ages (cal yr BP)													
			i-GS1	o-GS1	i-GS2	o-GS2	i-GS1			o-GS1			i-GS2			o-GS2				
							Median	2 $\sigma$ range	Median	2 $\sigma$ range	Median	2 $\sigma$ range	Median	2 $\sigma$ range	Median	2 $\sigma$ range	Median	2 $\sigma$ range		
3	1 D03-B18	BE-20805, 20806, 20807, 20808	4306 ± 31	2450 ± 30	1404 ± 29	399 ± 29	4413	4175	4639	2089	1891	2299	787	923	738	1104	<i>overlapped post-1950</i>			
	2 D03-BL	KIA-52291	4002 ± 25				4009	3803	4236											
	3 D03-BR	KIA-52290	3293 ± 26				3121	2916	3331											
	4 D03-C	KIA-53649, 53650	3174 ± 27				444 ± 23	2969	2766	3169								<i>overlapped post-1950</i>		
	5 D03-B12	BE-20793, 20794, 20795, 20796	3170 ± 31	2504 ± 30	1316 ± 29	511 ± 29	2965	2761	3167	2158	1950	2339	955	831	665	995	114	0	258	
	6 D03-C	KIA-53651, 53652	3036 ± 26				1925 ± 25	2810	2635	3012								1456	1286	1635
	7 D03-B15	BE-20797, 20798, 20799, 20800	2726 ± 30	2028 ± 30	1'35 ± 30	931 ± 29	2443	2252	2682	1574	1377	1760	452	757	608	925	501	335	642	
	8 D03-B114	BE-20809, 20810, 20811, 20812	2210 ± 30	2032 ± 30	1448 ± 30	839 ± 29	1790	1589	1987	1579	1382	1766	225	972	787	1157	419	259	558	
	9 D03-B17	BE-20801, 20802, 20803, 20804	1277 ± 29	642 ± 29	498 ± 29	454 ± 29	796	643	954	231	41	422		105	0	251	<i>overlapped post-1950</i>			

\*Leibniz Labor, Kiel (lab code KIA). \*\*LARA, Bern (lab code BE); i-GS1, inner Growth Stage 1; o-GS1, outer Growth Stage 1; i-GS2, inner Growth Stage 2; o-GS2, outer Growth Stage 2;  $\Delta o1-i2$ , hiatus between o-GS1 and i-GS2. #Calculated using the Marine20 curve (Heaton et al., 2020) and a weighted average  $\Delta R = -133 \pm 52$  from Amami-o-jima (Yoneda et al., 2007) and Kikai-jima (Hirabayashi et al., 2017). 1–9, specimen reference number in Fig. 7.

**Table 2**

Mean annual palaeo-SST (°C) and inferred palaeotemperatures at 75–100 m water depth for the sampled localities. Calibrated ages calculated with the Marine20 curve (Heaton et al., 2020) and a weighted  $\Delta R$  of  $-133 \pm 52$  from Amami-o-shima (Yoneda et al., 2007) and Kikai-jima (Hirabayashi et al., 2017).

References	Conventional $^{14}\text{C}$ age (years BP)	Calibrated $^{14}\text{C}$ age (cal yr BP) Median [2 $\sigma$ range]	palaeo-SST (at 0–10 m, 1 $\sigma$ range)	Inferred palaeotemperature (at 75–100 m, 1 $\sigma$ range)
Abram et al. (2001)	$4220 \pm 70$	4297 [4007–4568]	21.5–22.1 $^{\$}$	19.4–20.7
Abram et al. (2001)	$3790 \pm 70$	3729 [3455–3989]	20.1–21.0 $^{\$}$	18.0–19.6
Chuang et al. (2023)	$3595 \pm 20$	3486 [3307–3688]	22.4–22.9 $^{\$}$	20.3–21.5
Abram et al. (2001)	$3360 \pm 20$	3207 [2998–3387]		
Garas et al. (2023)	$3400 \pm 70$	3251 [2978–3487]	19.3–20.3 $^{\$}$	17.2–18.9
Abram et al. (2001)	$3235 \pm 20$	3047 [2841–3250]	20.5–21.3 $^{\$}$	18.4–19.9
Abram et al. (2001)	$1860 \pm 70$	1395 [1175–1619]	21.5–22.1 $^{\$}$	19.4–20.7
Kawakubo et al. (2017) *		AD 1570–2010	$24.5 \pm 1.2$	21.2–24.3
JODC **		AD 1906–2003	24.5	22.4–23.1

\* Estimated from modern coral Sr/Ca records.

\*\* Japan Oceanographic Data Center (available at <http://www.jodc.go.jp/>).

$^{\$}$  Calculated from annual averages of fossil (Abram et al., 2001; Garas et al., 2023; Chuang et al., 2023) and modern (Kiyama et al., 2000; Morimoto et al., 2007; Kajita et al., 2017) coral  $\delta^{18}\text{O}$  values using a temperature dependency of  $-0.20 \pm 0.02 \text{‰}/^{\circ}\text{C}$  (Juillet-Leclerc and Schmidt, 2001).

carbonates (e.g., larger benthic foraminifera, fragments of live and dead corals; Matsuda et al., 2010, 2011). The shelf is bathed by clear, oceanic waters of normal salinities and an average annual sea surface temperature (SST) of  $24.6 \text{ }^{\circ}\text{C}$  (data from <http://www.jodc.go.jp/service.htm>). The assessed water speed on the Kikai-jima shelf at c. 100 m depth is c.  $10 \text{ cm/s}$  (Nakamura et al., 2007). Terrigenous sediments derived from Amami-o-shima, located to the northwest, are trapped in submarine channels between the two islands, and the sedimentation rate is low in the study area (Arai et al., 2008).

### 3. Materials and methods

#### 3.1. Morphology and bioerosion analysis

The studied macroids were dredged from the transect D-03 on the main WE2 transect line on a flat seafloor (mobile sandy and gravelly bioclastic carbonates) south-west of Kikai-jima ( $28^{\circ}14'\text{N}$ ,  $129^{\circ}50'\text{E}$ ; Bassi et al., 2012; Fig. 1). The transect D-03 ranges from 75 to 100 m water depth. After washing and drying just after acquisition, outer surfaces and sectioned polished surfaces of the macroids were analysed with a binocular microscope at Tohoku University. The analysis of the macroid sphericity was performed by measuring the shorter, larger, and intermediate axes of 24 macroid specimens, from which the shorter, larger, and intermediate axes of the distinguished growth stages were also assessed. The data were plotted in ternary diagrams using the TRIPLOT spreadsheet (Graham and Midgley, 2000). Growth-form terminology follows that proposed by Woelkerling et al. (1993).

Bioerosion traces and macroid inner arrangement were studied on polished macroid slabs sectioned along the plane, including the centre of the specimen (Bassi et al., 2011, 2012). Macroid inner arrangements were qualitatively assessed on specimen slabs. Both halves of macroids were scanned at a resolution of 2400 dpi. The definitions of inner arrangement of nodules follows Bosellini and Ginsburg (1971) and Bosence and Pedley (1982). The amount of boring with respect to the original macroid volume was defined by the bioerosion index (BI; Bassi et al., 2012). Proportions of constructional voids (e.g., Minnery, 1990; Nitsch et al., 2015) were also estimated. Taxonomy of encrusting foraminifera follows Perrin (1987, 1994, 2009) for *Acervulina inhaerens*, and Krautwig et al. (1998) for *Homotrema rubrum* and *Miniacina miniacea*. The studied material is deposited at the Institute of Geology and Paleontology, Graduate School of Science, Tohoku University, Sendai.

#### 3.2. Radiocarbon dating

Radiocarbon dating was performed on nine macroid specimens. All macroid nuclei (i.e., acervulinid test) were dated. The external (within a

thickness of  $<1 \text{ mm}$ ) surfaces were dated in seven macroids. All specimens showed growth stages, and the external part of the first growth stage and the internal part of the second growth stage were dated in five macroids (Table 1).

The radiocarbon measurements on nine Kikai-jima macroids (Table 1) were performed by two different  $^{14}\text{C}$  laboratories (Table 1). In total six analyses of four macroids were conducted at the Leibniz Labor für Altersbestimmung und Isotopenforschung (KIA) at the Christian-Albrechts University, Kiel, Germany. The measurements were conducted using the type HVE 3MV Tandetron 4130 accelerator mass spectrometer (AMS). The  $^{14}\text{C}/^{12}\text{C}$  and  $^{13}\text{C}/^{12}\text{C}$  isotope ratios were simultaneously measured by the AMS, compared to the  $\text{CO}_2$  measurement standards and corrected for effects of exposure to foreign carbon during the sample pre-treatment. The reported uncertainty of the  $^{14}\text{C}$  result takes into account the uncertainty of the measured  $^{14}\text{C}/^{12}\text{C}$  ratios of sample and measurement standard, the uncertainty of the fractionation correction and the uncertainty of the applied blank correction. In total, 20 analyses of five macroids were performed at the Laboratory for the Analysis of Radiocarbon with AMS (LARA) at the University of Bern, Switzerland using a 200 kV MICADAS instrument. In order to guarantee traceability of the results, the  $^{14}\text{C}$ -free standard IAEA-C1 and the primary standard IAEA-C2 were used for blank subtraction, standard normalization, and correction for isotope fractionations. Sample treatment of marine carbonates,  $^{14}\text{C}$  analysis and determination of appropriate measurement uncertainties were validated by Gottschalk et al. (2018).

The dates, along with the Kikai-jima coral datations provided by Webster et al. (1998) and Sugihara et al. (2003), were calibrated to calendar years (cal yr BP) using the Marine20 curve (Heaton et al., 2020) and a local reservoir effect of the weighted average  $\Delta R$  of  $-133 \pm 52$  (2 $\sigma$ ) from Amami-o-shima (Yoneda et al., 2007) and Kikai-jima (Hirabayashi et al., 2017; Table 1).

#### 3.3. Water temperature assessment

The vertical profile from 0 to 200 m of annual mean temperatures for 1906–2003 off Kikai-jima ( $28^{\circ}–29^{\circ}\text{N}$ ,  $129^{\circ}–130^{\circ}\text{E}$ ) was reconstructed with data from the Japan Oceanographic Data Center (JODC; <http://www.jodc.go.jp/>). Although the Ryukyu Islands have been under the influence of interannual-to-interdecadal climate variabilities such as the East Asian Monsoon, ENSO, and Pacific Decadal Oscillation since the Middle-to-Late Holocene (Kawakubo et al., 2017; Asami et al., 2020; Garas et al., 2023), the mean climate state was almost stable on a centennial-to-millennium timescale (Chuang et al., 2023). The present-day vertical profile of seawater temperature has been almost/likely constant in gradient during the Late Holocene (Li et al., 2020). The

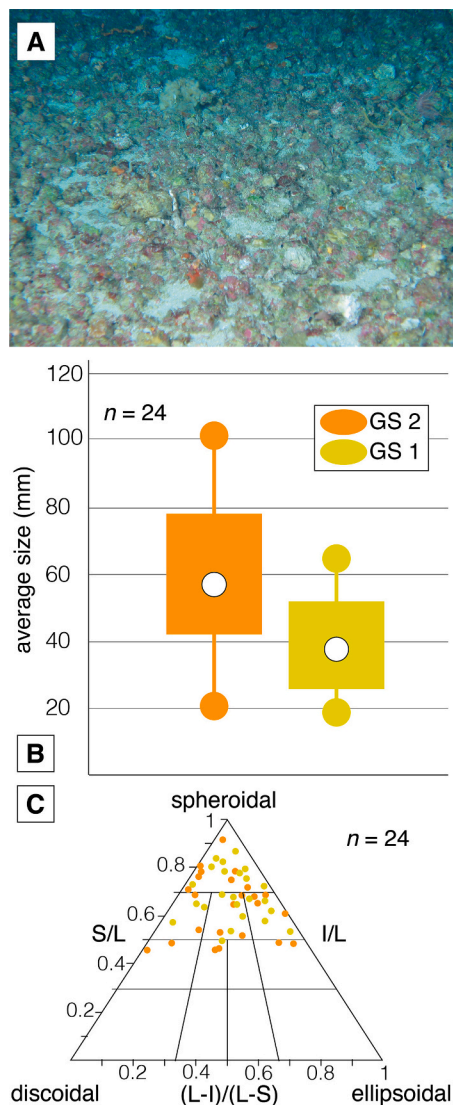


**Fig. 2.** Macroid morphology. A, field photograph of the rhodolith bed at c. 120 m water depth on the Miyako-Sone submarine platform showing some nodules covered by encrusting sponges (red, yellow and orange) along with greenish coatings of microbial mats. B, box plot showing the average size of 38 mm (average size range) for the GS1 and of 58 mm for the GS2 of the measured macroid specimens;  $n = 24$ . C, the macroid growth stages are spheroidal–sub-spheroidal in shape (axes: shorter, S; larger, L; intermediate, I). GS1, first growth stage; GS2, second growth stage. (For interpretation of the references to colour in this figure legend, the reader is referred to the web version of this article.)

palaeotemperature ranges at 75–100 m depth were assessed from the palaeo-SST reconstructions from oxygen isotope ( $\delta^{18}\text{O}$ ) records of modern and fossil corals from Kikai-jima (Kiyama et al., 2000; Abram et al., 2001; Morimoto et al., 2007; Kajita et al., 2017; Garas et al., 2023; Chuang et al., 2023) for the time slices of 4568–4007, 3989–3455, 3688–2998, 3487–2978, 3250–2841, and 1619–1175 cal yr BP ( $2\sigma$ ) (Table 2). Hereafter the median ages are referred as 4300, 3700, 3500–3200, 3300, 3000, and 1400 cal yr BP, respectively.

## 4. Results

### 4.1. Macroid shape and inner arrangement

Maximum diameter of the studied macroids ( $n = 24$ ) ranges between 25 mm and 130 mm (average 71.6 mm, standard deviation s.d. 27.7

mm), the intermediate diameter ranges from 19 to 93 mm (average 58.2 mm, s.d. 23.1 mm), and the minimum diameter ranges from 12 to 89 mm (average 46.7 mm, s.d. 21.8 mm; Fig. 2). Dominating shapes are spheroidal and sub-spheroidal with asymmetric concentric inner arrangement (Figs. 3–6). The outer surface mainly shows encrusting *Acervulina inhaerens* and subordinate thin encrusting hapalidialean coralline red algae (*Lithothamnion* sp.). Common warty and rare lumpy acervulinid growths are also present (Fig. 3). Rare warty thin corallines, most still living when collected, bryozoans and serpulids are also present. The nuclei of the macroids consist of small bivalve and older macroid fragments. The asymmetric concentric inner arrangement consists of superimposed encrusting *Acervulina inhaerens* specimens intergrown with subordinate coralline algae and a high volume of constructional voids. Subordinate components are serpulids, bryozoans, and the foraminifera *Homotrema rubrum* and *Miniacina miniacea*.

Two distinct stages of growth, marked by abraded and bioeroded surfaces, can be distinguished in all studied macroids (Figs. 4–6). The longest axis of the first growth stage (GS1) around the nucleus is 63 mm, and the mean diameter ranges from 26 mm to 52 mm (average 39 mm; Fig. 2B). The second growth stage (GS2) completes the dimensions of the entire macroid specimens (Fig. 2B). GS2 shapes are inherited from GS1 ones (Fig. 2C). The macroids were heavily bored in both growth stages (BI is 3) commonly by sponges (*Entobia* isp.), sipunculid and polychaete worms (*Maeandropolydora* isp., *Trypanites* isp.), and commonly to rarely by bivalves (*Gastrochaenolites* isp.), algae, cyanobacteria, and fungi (microborings). The boundary between GS1 and GS2 is characterized by an abraded surface deeply colonized mainly by *Entobia* isp. showing a comparable degree of abrasion in all macroids. In the GS2, *Gastrochaenolites* isp. can be common. The chemical mytilid borers *Leiosolenus* sp. and *Lithophaga* sp. were identified within the traces (Bassi et al., 2020). In both stages, borings and constructional voids have no sediment infilling (Figs. 4–6).

### 4.2. Macroid ages and water temperatures

The radiocarbon datings of the macroid inner (GS1) parts (acervulinid tests) gave an oldest age of 4413 cal yr BP (4175–4639 cal yr BP) and a youngest age of 796 cal yr BP (643–954 cal yr BP). The outer stages of the macroids (GS2) yielded an oldest age of 1456 cal yr BP (1286–1635 cal yr BP) and youngest ones ranging from 114 cal yr BP (0–258 cal yr BP) to present-day (Table 1, Fig. 7). The two distinguished growth stages are separated by hiatuses ranging from 955 to 225 years (Table 1).

The vertical profile of present-day annual mean temperature off Kikai-jima shows a SST of c. 24.5 °C and values of c. 23.1–22.4 °C at the sampled macroid beds (75–100 m water depth) (Table 2, Fig. 8). The palaeo-SST estimated from Kikai-jima corals varies from 21.5 to 22.1 °C at c. 4300 cal yr BP to 20.1–21.0 °C at c. 3730 cal yr BP (Abram et al., 2001; Table 2, Fig. 8). At c. 3200 cal yr BP palaeo-SST ranged from 19.3 to 22.9 °C (Abram et al., 2001; Garas et al., 2023; Chuang et al., 2023; Table 2). Paleo-SST was 21.5–22.1 °C at c. 1400 cal yr BP (Abram et al., 2001). Modern SST values were reached since the 1570 CE (24.5 ± 1.2 °C; Kawakubo et al., 2017). At the sampled water depths, the inferred palaeotemperatures show minimum values at c. 3250 cal yr BP (17.2–18.9 °C) and maximum values in recent times at 1570–2010 CE (21.2–24.3 °C; Table 2).

## 5. Discussion

The studied macroids clearly formed *in situ* on the flat island shelf southwest off Kikai-jima. The mobile sandy and gravelly bioclastic carbonates deposited on hard rocky substrates (e.g., Matsuda et al., 2011) were inhabited by the acervulinid community at least since the latest Middle Holocene as evidenced by the age estimations of the earliest acervulinid growth (between c. 4300 and c. 1277 cal yr BP; Table 1). The acervulinid and crustose coralline algal covers of the

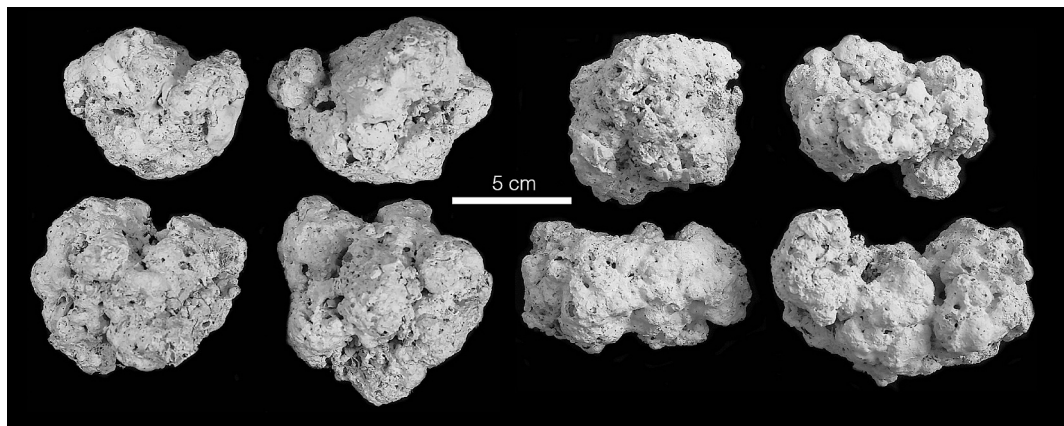


**Fig. 3.** Outer surfaces of macrooids showing the encrusting acervulinid growth forms; 75–100 m water depth, off Kikai-jima, Central Ryukyu Islands, Japan.

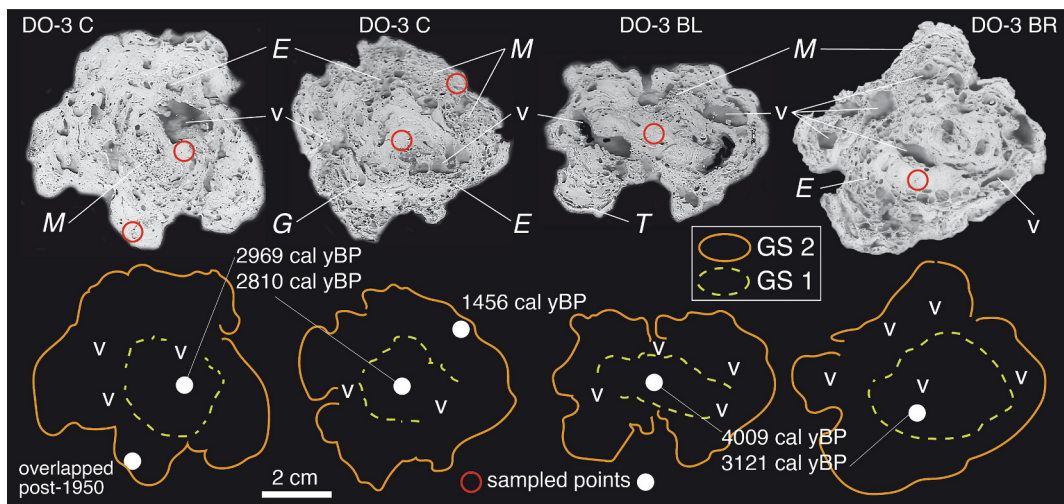


**Fig. 4.** Slab surfaces of macrooids showing a complex inner arrangement, boring patterns and locations of the radiocarbon dating (Table 1); 75–100 m water depth, off Kikai-jima, Central Ryukyu Islands, Japan. E, *Entobia* isp.; G, *Gastrochaenolites* isp.; M, *Maeandropolydora* isp.; T, *Trypanites* isp.; v, void; GS1, first growth stage; GS2, second growth stage; cal yBP, calibrate years BP.

macrooids are still living.

### 5.1. Environmental conditions of growth

Previous studies have shown that acervulinid foraminifera indicate reduced competition for substrate encrustation, which is one of the most critical factors controlling the biotic composition of epilithic benthic communities (Reiss and Hottinger, 1984; Walker et al., 2011). The first species encrusting a hard substrate can maintain their spatial distribution by the niche incumbency effect (Walker et al., 2011). *Acervulina inhaerens* can exclude other encrusting organisms and resist the invasion of new taxa over time, an ecological tendency observed in the Red Sea (Hottinger, 1983).

Reduced competition for substrate encrustation is related to a decrease in sedimentation rate (e.g., Taylor and Wilson, 2003), water turbulence (e.g., Taylor and Wilson, 2003; Aguirre et al., 2017) and irradiance (e.g., Reiss and Hottinger, 1984; Perrin, 1992; Perry and Hepburn, 2008). The setting of Kikai-jima macrooids is characterized by low sedimentation rates, which are revealed by the high bioerosion index (BI of 3) for both growth stages (Figs. 4–6). The dense bioerosion points to a long residence time of macrooids on mobile sandy and gravelly bioclastic carbonate substrate, allowing the boring organisms to thrive (Bassi et al., 2011, 2020). Specifically, low sedimentation rates are corroborated by the occurrence of microbioerosion (i.e., algae,

cyanobacteria, and fungi) made by heterotrophic microborers (Vogel et al., 2000; Golubic and Radtke, 2005), the dominance of *Entobia* made by etching sponges, and subordinately by polychaete worms (i.e., *Maeandropolydora*; e.g., Bromley, 1994), and characteristic boring bivalves (i.e., *Gastrochaenolites*; Bassi et al., 2020).

Ecological and palaeoecological interpretations of modern and fossil macroid/rhodolith deposits suggest that shape (i.e., sphericity) is not necessarily linked to water turbulence (Lund et al., 2000; Bassi et al., 2006; Steller et al., 2009; Aguirre et al., 2017; O'Connell et al., 2021). The studied spheroidal and sub-spheroidal macroids, which occur in an area swept by low-speed currents (Nakamura et al., 2007), confirm that there is no relationship between macroid sphericity and water energy/hydrodynamic setting, as concluded for the rhodoliths (Lund et al., 2000; Aguirre et al., 2017). The encrusting growth forms shown by all coralline algae making up the studied macroids have been interpreted as forming in calm waters (e.g., Adey and Macintyre, 1973; Braga and Martín, 1988; Bassi, 1995; Bosence, 1991a, 1991b; Perrin, 1992).

The asymmetric concentric inner arrangement of superimposed encrusting acervulinids suggests different growth stages with different increments (Williams et al., 2019). These were influenced by the long residence time on the seafloor rather than by the acervulinid growth rate.

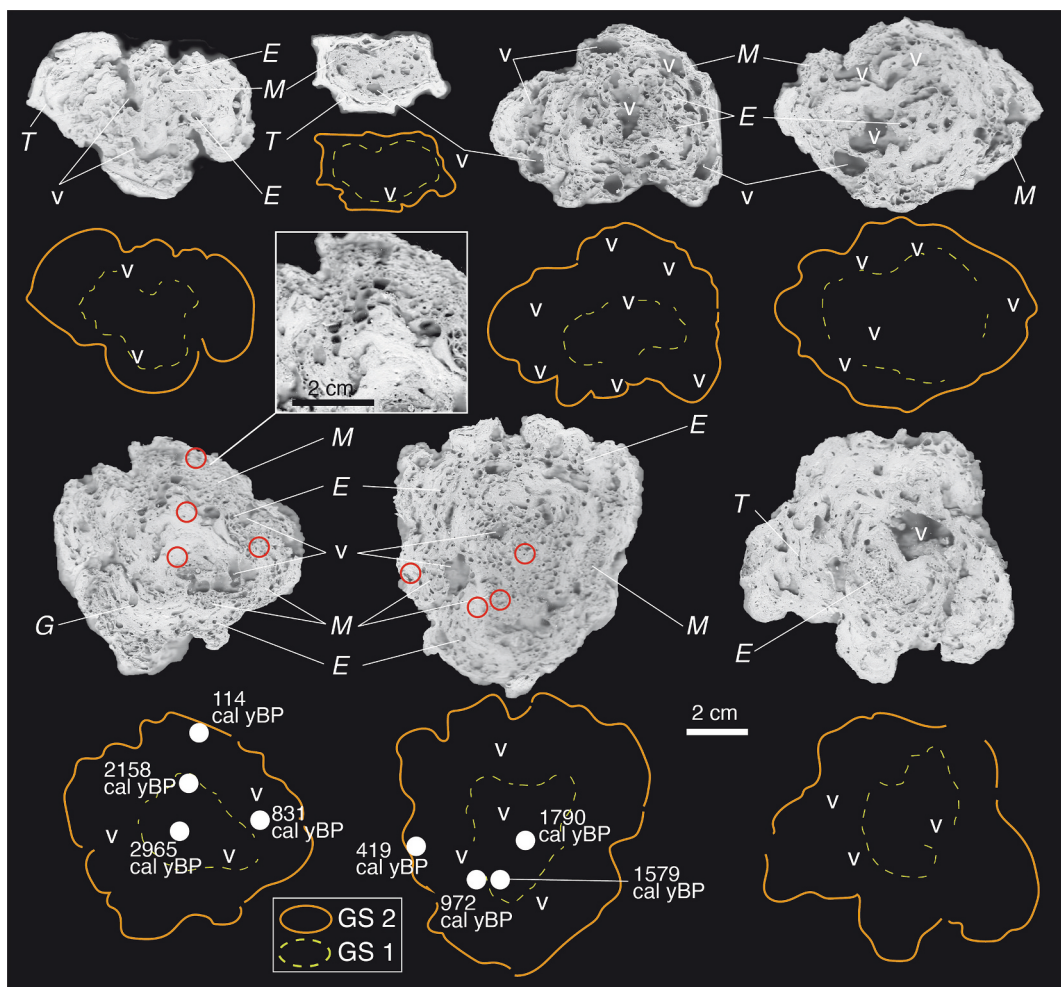


**Fig. 5.** Slab surfaces of macrooids showing a complex inner arrangement, boring patterns and locations of the radiocarbon dating (Table 1); 75–100 m water depth, off Kikai-jima, Central Ryukyu Islands, Japan. E, *Entobia* isp.; G, *Gastrochaenolites* isp.; M, *Maeandropolydora* isp.; T, *Trypanites* isp.; v, void; GS1, first growth stage; GS2, second growth stage; cal yBP, calibrate years BP.

### 5.2. Influence of temperature and irradiance on acervulinid growth

The Kikai-jima macrooids experienced temperature changes of c. 4.7 °C for c. 4400 years (i.e., c. 18 °C minimum at c. 3700 cal yr BP, 22.75 °C maximum of today; Fig. 8, Table 2), but the interruptions of growth of the macrooids do not show correlation with the three most recent cooling events with amplitudes of c. 1–2 °C, at around 1700, 3200 and 4400 cal yr BP (Wan et al., 2023; Fig. 7).

The mean climate state around Kikai-jima has been almost stable on a centennial-to-millennial timescale during the Middle to Late Holocene (Chuang et al., 2023). Reconstructed subsurface temperatures showed a small variability of c. 1.5 °C in the Okinawa Trough during the Late Holocene (Li et al., 2020). Because the variation of annual insolation at 30°N has been quite small (c. 1 W/m<sup>2</sup>) during the last 4400 years (Berger and Loutre, 1991), the estimated range (c. 4.7 °C) of seawater temperature variations inferred from paleo-SST data of massive *Porites* corals (Abram et al., 2001; Garas et al., 2023; Kawakubo et al., 2017; Table 2) can be considered as the maximum range of temperature change in Kikai-jima waters during the latest Middle to Late Holocene.

The absence of hermatypic corals and the subordinate role of coralline red algae and larger foraminifera suggest that low irradiance favoured the acervulinid dominance in macroid beds, since light deficiency is a discriminating factor between encrusting foraminifera and major reef-building organisms (Reiss and Hottinger, 1984; Perrin, 1992; Perry and Hepburn, 2008; Kawahata et al., 2019). Although the absence

of symbionts in acervulinids is not fully confirmed (Leutenegger, 1984; Perrin, 1992), low light irradiance is an important factor favouring the dominance of acervulinids which thrive in less bright areas than photophyle organisms on hard substrates (Hottinger and Levinson, 1978; Palmieri and Jell, 1985; Perrin, 1992). Although thin encrusting *Lithothamnion* sp. and other halapalidialeans are common in relatively deep-water settings (e.g., Adey et al., 1982; Minnery, 1990; Iryu et al., 1995; Lund et al., 2000; Littler and Littler, 2003), low irradiance probably reduced their ability to compete for substrate incrustation with acervulinids.

### 5.3. Interrupted growth of acervulinids

The nuclei of the GS1 yielded ages of c. 4400–796 cal yr BP, whereas the dated outer growth stages range from c. 1456 cal yr BP to present-day (Table 1). A significant difference in age between the two distinguished growth stages was found in all dated nodules, indicating that their active growth was interrupted for long time spans (Fig. 9).

The GS1–GS2 boundary is characterized by an abraded rugged surface deeply colonized by mainly *Entobia* isp. This hiatus/time gap ranges from c. 955 to 225 cal yr BP (Table 1). Ages of the macroid nuclei, interruptions of growth (i.e., outer GS1) and the hiatuses between the two growth stages show neither a specific temporal pattern nor synchronicity (Fig. 7).

Each individual macroid, after a long period of growth interruption

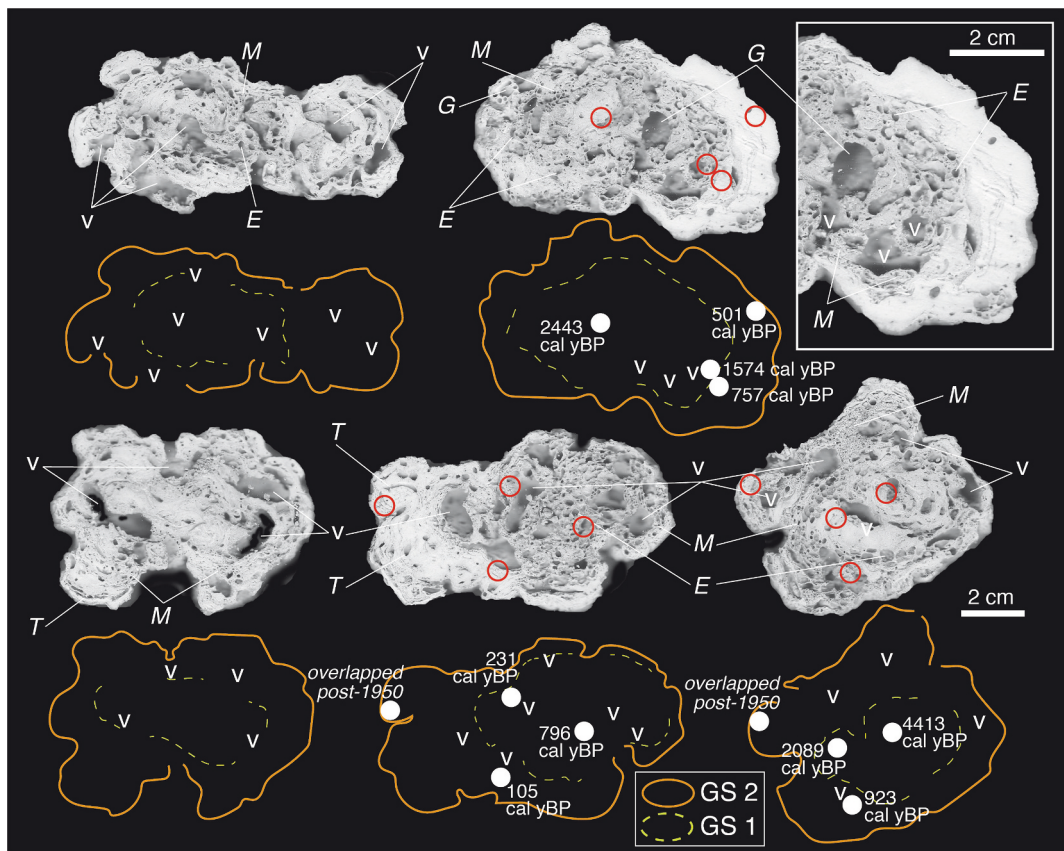


**Fig. 6.** Slab surfaces of macroids showing a complex inner arrangement, boring patterns and locations of the radiocarbon dating (Table 1); 75–100 m water depth, off Kikai-jima, Central Ryukyu Islands, Japan. E, *Entobia* isp.; G, *Gastrochaenolites* isp.; M, *Maeandropolydora* isp.; T, *Trypanites* isp.; v, void; GS1, first growth stage; GS2, second growth stage; cal yBP, calibrate years BP.

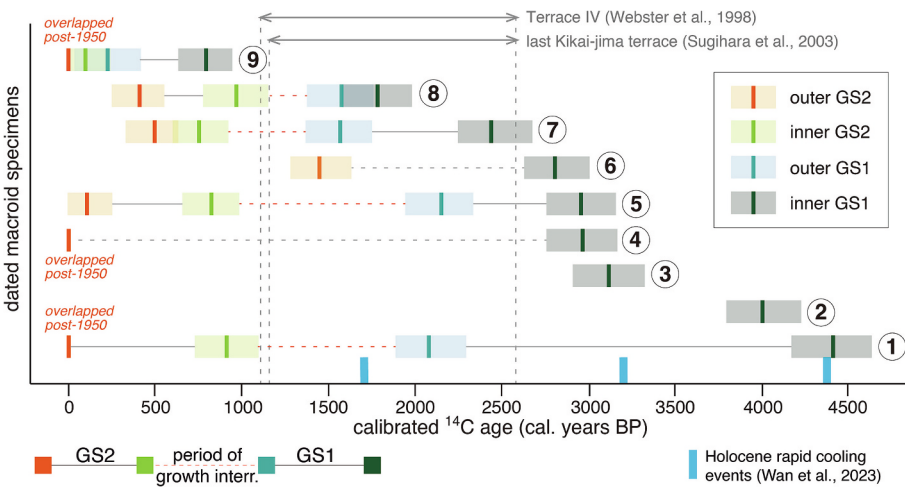


**Fig. 7.** The nine radiocarbon-dated acervulinid macroids show different ages from the core (inner GS1) to the outer surfaces (outer GS2). There is a long (up to c. 1000 years; Table 1) and highly varying hiatus (growth interruption) between the two distinguished growth stages (i.e., outer GS1, inner GS2) in different macroid individuals. Holocene rapid cooling events with amplitudes of c. 1–2 °C (Wan et al., 2023) did not affect macroid growth. No giant tsunami have been so far identified (Fujiwara et al., 2020). Other events identified in the Kikai-jima area (e.g., uplift of terrace IV, Webster et al., 1998; last Kikai-jima terrace, Sugihara et al., 2003) do not correlate with macroid growth interruptions. For each studied macroid specimen rectangle widths and bold vertical lines are  $^{14}\text{C}$  2- $\sigma$  ranges and median respectively (Table 1).

due to harsh ecological conditions for the acervulinids, shows a subsequent ecological restoration which gave rise to the GS2 (Figs. 4–6), in which the acervulinids started again to grow and the macroid was again colonized by skeletal epizoans (i.e., serpulids, bryozoans), boring organisms, and epiphytes (corallines). Despite the favourable setting (i.e.,

low sedimentation rate), after a first growth stage, each individual macroid suffered a long-lasting growth interruption and a subsequent regrowth at times different from those of its neighbours (Fig. 9).

Encrusting acervulinids need a relatively stable substrate with a low sedimentation rate to avoid burial. Below the fair-weather wave base, as

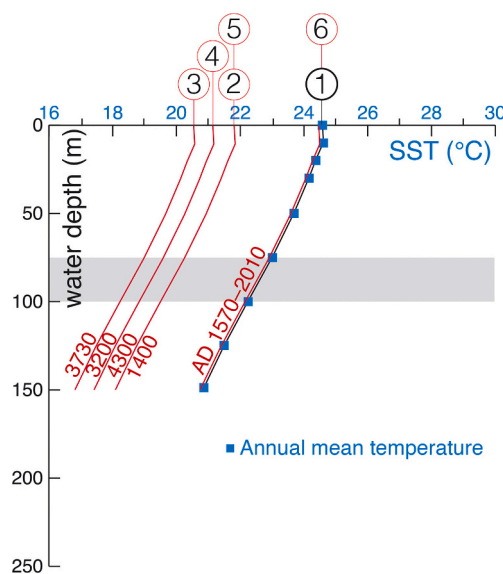


**Fig. 8.** Vertical profiles of annual mean temperature of sea water off Kikai-jima. Profile 1 shows present-day data from Data Online Service System (JODC) provided by Japan Oceanographic Data Center (<http://www.jodc.go.jp/>) and from Kawakubo et al. (2017). The grey area marks water depth of studied macrooids. Profiles 2–6 (red) are assessed considering the present-day vertical profile gradient (1) and the estimated palaeo-SSTs (see Table 2). 2, 4300 cal yr BP (Abram et al., 2001); 3, 3730 cal yr BP (Abram et al., 2001); 4, 3200 cal yr BP (Abram et al., 2001; Garas et al., 2023; Chuang et al., 2023); 5, 1400 cal yr BP (Abram et al., 2001); 6, 1570–2010 CE (Kawakubo et al., 2017). (For interpretation of the references to colour in this figure legend, the reader is referred to the web version of this article.)

in this case study, the higher stability of the macroids allows the acervulinid assemblage to thrive longer (e.g., Matsuda and Iryu, 2011; Bassi et al., 2012, 2013). However, an ecological condition produced the interruption of the acervulinid/macroid growth. Such condition did not affect the whole macroid bed but individual macroids, as demonstrated by the different durations of the hiatus between the growth stages and the absence of growth synchronicity (Fig. 7; Table 1).

To date, two possible types of factors have been suggested for causing growth interruption in rhodoliths made up of coralline algae in quiet conditions below the fair-weather wave base (e.g., Prager and Ginsburg, 1989; Aguirre et al., 2017; Vale et al., 2018). One of these types is

increased sedimentation rate and/or increased turbidity, which can be related to catastrophic events (i.e., occasional severe storms, tsunamis) that affect rhodolith accumulations (e.g., Braga and Martín, 1988; Steller and Foster, 1995; Smith and Cooper, 2004; Tâmega et al., 2014; Puga-Bernabéu and Aguirre, 2017; Johnson et al., 2017; Lavenère-Wanderley et al., 2021). Kikai-jima, located on the actively subducting Amami Plateau (Kato, 1993), underwent several meter-scale uplift events in the last 2000 years (Shimazaki and Nakata, 1980; Kawana, 1989; Webster et al., 1998; Ota et al., 1978, 2000; Sugihara et al., 2003; Fig. 7). However, despite these events have been characterized by quick and repeated large earthquakes, by relatively small earthquakes or by stable uplift without large earthquakes (Nakata et al., 1978; Goto, 2017), they probably did not generate large tsunamis (Fujiwara et al., 2020) since tsunami-related deposits have not been identified so far in the Kikai-jima area.

On the other hand, the overturn and burying of rhodoliths with subsequent growth interruption can be caused by the biogenic mobilization of rhodoliths by vagrant organisms (e.g., *Malachanthus plumieri*) moving around algal nodules (Marrack, 1999; Amado-Filho et al., 2012).

These two types of factors act at different spatiotemporal scales. The first affects the whole bed simultaneously, whereas the second represents an occasional event for individual macroids. Because Kikai-jima macroids show no synchronous growth interruption, which otherwise occurs in all studied specimens, most probably random biogenic processes are responsible for interruptions of macroid growth.

#### 5.4. Deterring mechanism in growing acervulinids and settlement of surface-colonizing organisms

A potential third factor producing the acervulinid growth interruption might be related to the temporal occupation of the macroid surface by organisms or biofilms that do not leave calcareous skeletal remains for nodule accretion. In particular, sponges and biofilms might have antifouling properties preventing acervulinid growth, epiphytes and boring bivalve settlement on macroid surfaces. Microbial biofilms play important roles in initiating settlement of marine invertebrate larvae. Laboratory studies showed that biofilms contributed to the settlement of sponge larvae, with markedly higher numbers of larvae settling on biofilms (Whalan and Webster, 2014). Marine bacteria forming biofilms can produce compounds with algicidal and anti-epifaunal properties (Bowman, 2007; Gomez-Lemos and Diaz-Pulido, 2017). Sponges rely

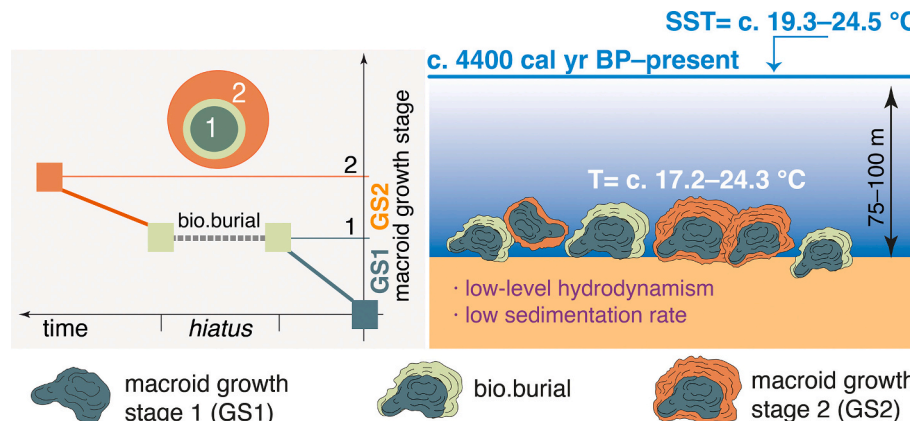


**Fig. 9.** Model of individual macroid growth. The macroid inner arrangements (i.e., asymmetric concentric arrangement with high proportions of constructional voids) point to low sedimentation rate and low-level hydrodynamic conditions in the depositional setting. Macroids, initially grew c. 4400 yrs. ago at c. 20.0 °C water temperature (Table 2). They show two growth phases (GS1, GS2) separated by an interruption of acervulinid growth (hiatus; grey dashed line) marked by an abraded surface deeply colonized by mainly *Entobia* isp., which points to a long residence time on the sea floor. Temporal occupation of the macroid surface by soft-bodied organisms and/or biofilms and random biogenic mobilization and occasional burial (bio.burial) of single macroid specimens caused macroid growth interruption. Subsequent re-colonization of nodule by acervulinids built the GS2s. This stage lasts until today with living coralline algal and acervulinid covers. Sketch, not to scale.

**Table 3**

Location, age, features and setting of reported Cretaceous–Miocene acervulinid assemblages.

Reference	Location	Age	Feature	Setting
Caratelli et al. (2021)	N Patagonia	Early Cretaceous	macroids	proximal outer ramp
Robless-Salcedo et al. (2013)	NE Spain	late Campanian–early Maastrichtian	encrusting	reef
Beckmann et al. (1982)	NW Italy	Campanian–Paleocene	encrusting	shallow-water platform
Baceta et al. (2005)	N Spain	Danian	encrusting	patch and barrier reefs
Schlagintweit et al. (2018)	Austria	Danian	encrusting	shallow-water platform
Elliott (1964)	Spanish Pyrenees, Slovakia, Iraq, Arabia, Pakistan	early Eocene	encrusting	shallow-water platform
Plaziat and Perrin (1992)	S France, N Spain	early Ypresian	encrusting, branching, framestone	high turbidity reef slope-to-outer platform
Eichenseer and Luterbacher (1992)	NE Spain	early Ypresian	encrusting, macroids	reef mounds
Moussavian and Höfling (1993)	Austria, S France	early Eocene	encrusting, macroids	shallow-water platform
Scheibner et al. (2007)	NE Spain	early Eocene	encrusting, macroids	reef mounds
Tomás et al. (2016)	N Oman	early Eocene	encrusting, tubular	inner platform (seagrass)
Ferratges et al. (2021)	NE Spain	Ypresian	encrusting	middle platform
Perrin (1992, 1994, 2009)	N Spain, S France; Loyalty Islands	early Eocene; early Eocene	encrusting	inner platform
Rasser (1994)	Mururoa	Pleistocene–Recent		
Nebelsick et al. (2005)	Austria	Ypresian–Lutetian	encrusting, macroids	shallow-water (seagrass)
Martín-Martín et al. (2021)	Circumalpine area	middle Eocene	encrusting, macroids	proximal outer shelf
Pálfalvi (2004)	Hungary	middle Eocene	encrusting	inner ramp
Varrone and D'Atri (2007)	W Italy	Lutetian–Bartonian	macroids	deep infralittoral
Brandano and Tomassetti (2022)	NW Italy	Bartonian	encrusting, macroids	middle ramp
Coletti et al. (2021)	NW Italy	Bartonian–Priabonian	macroids	middle platform
Hagn and Wellnhofer (1967)	Bavaria	late Eocene	encrusting	inner platform
Darga (1993)	Bavaria	late Eocene	encrusting, macroids	middle ramp
Poisson and Poignant (1975)	W Antalya	Early Miocene	Encrusting, macroids	shallow-water platform
Karabiyikoglu et al. (2005)	W Antalya	Early–Middle Miocene	encrusting	coral patch-reefs
Wiedl et al. (2012)	Lower Austria	Middle Miocene	encrusting, macroids	shallow-water seagrass meadows
Aftabuzzaman et al. (2021)	Minamitorishima (Marcus Island)	Tortonian	encrusting	coral reef

heavily on the production of chemicals as a form of defence against predators, competitors, fouling organisms, and microbes (Maida et al., 1995; Suzuki et al., 1998; Krug, 2006). Interestingly, the compounds appear to be produced by associated microorganisms rather than the sponge (Taylor et al., 2007; Webster and Taylor, 2012). Some ascidians and/or harboured cyanobacteria produce bioactive compounds (Hamamoto and Reimer, 2022).

Images of the macroid bed on the Miyako-Sone submarine carbonate platform (c. 120 m water depth; Fig. 5c, Arai et al., 2014; Fig. 2A) show nodules totally or partially covered by sponges (red orange and yellow colours, may be ascidians as well) and other covered by greenish microbial mats (biofilms), indicating that acervulinids and coralline algae are absent from the nodule surface for certain periods of time. A similar situation is presumed for the Kikai-jima macroids.

The common *Entobia* bioerosions were made by boring sponges that colonize hard substrates (i.e., macroid surface) available after acervulinid death and experienced less space competition from weakened neighbouring organisms (e.g., boring bivalves). The end of the GS1 is in fact marked by a highly bioeroded surface by etching sponges (Figs. 4–6). In oligotrophic settings from the southern Caribbean Sea, the microbiome associated to *Cliona varians* aids the sponge to be able to colonize and bioerode in environments with low access and scarce availability of nitrogen sources (Sánchez-Suárez et al., 2022). Associated with the sponge's etching scars microbioerosions of algal, cyanobacterial and fungal origin has been interpreted as both eroding simultaneously and potentially even being engaged in a possible symbiotic relationship (Schönberg et al., 2019). The micro-endolithic traces identified in the studied macroids (Bassi et al., 2011, fig. 4) likely represent these microbioerosions.

## 6. Resilient Kikai-jima macroids and their fossil counterparts from the Western Tethys

The family Acervulinidae Schlotze, as re-assessed by Perrin (1994), includes several genera among which the systematically close-related genera *Acervulina* Schltze, 1854 and *Solenomeris* Douvillé, 1924 can form macroids and foraminiferal reefs (Perrin, 1992; Plaziat and Perrin, 1992). Both genera have fossil records: *Acervulina* is mainly reported from the Neogene to the Recent, whereas *Solenomeris* is known from the Early Cretaceous to Miocene (Perrin, 1994; Bassi, 2003; Caratelli et al., 2021). Acervulinid framestones and macroids have been mainly described from the early (Ypresian) and middle (Bartonian) Eocene of the Western Tethys (Table 3). Three records are from the Early and Middle Miocene (Poisson and Poignant, 1975; Karabiyikoglu et al., 2005; Wiedl et al., 2012) and one in the Late Miocene (Aftabuzzaman et al., 2021). Fossil acervulinid framestones and macroids formed in middle ramp settings with rare occurrences in inner- and outer-ramp areas (Table 3).

Between the Paleocene–Eocene Thermal Maximum (PETM; McInerney and Wing, 2011) and the rapid growth of ice on Antarctica in the earliest icehouse state of the Oligocene (Anagnostou et al., 2016), the long-term cooling trend was interrupted by a short-warming event known as the Middle Eocene Climatic Optimum (MECO; Henehan et al., 2020). The stratigraphical occurrences of abundant acervulinid accumulations coincide with the PETM and the MECO. According to our results, the flourishing of acervulinids is likely due to almost no competition for space by phototrophic organisms (i.e., hermatypic corals, coralline red algae, larger foraminifera) in the low light settings in which they thrived.

The PETM and MECO warming events lasting c. 200–400 kyr with a rapid global warming (5–8 °C; e.g., McInerney and Wing, 2011; Henehan et al., 2020) did not directly contribute to the flourishing of the

acervulinids which, instead, are independent of such temperature variations, as shown by the Kikai-jima macroids. The thick encrusting acervulinid and macroid accumulations demonstrate that conditions favourable to acervulinids can persist for thousands of years. In middle ramp settings, below the fair-weather wave base (Table 3), acervulinids can thrive in low-irradiance settings and become dominant organisms over the phototrophic ones.

In Kikai-jima shelf, no significant nutrient input or flux of particulate organic matter is known. Macroids beds flourish in oligo-mesotrophic conditions, also promoting highly diversified Okinawa coral reef and larger benthic foraminiferal communities (e.g., Hohenegger, 1999; Ministry of the Environment and Japanese Coral Reef Society, 2004; Iryu et al., 2006; Sinniger et al., 2019; Takeyasu et al., 2023). The Kikai-jima macroids do not support the interpretation of acervulinids as opportunistic foraminiferal indicators of eutrophic environments (Schlagintweit et al., 2018) and contradict that acervulinids might indicate deterioration of trophic conditions, suggested as the cause for the sifting in Eocene shallow-water carbonate producers from zoanthellate corals and larger foraminifera to encrusting foraminifera and coralline algae (Brandano and Tomassetti, 2022).

## 7. Concluding remarks

Internal morphology, bioerosion patterns, and radiocarbon datings of living acervulinid macroids collected at 75–100 m water depth on the shelf off Kikai-jima (Central Ryukyu Islands, Japan) suggest that they have been growing for thousands of years with long periods of growth interruption.

The examined specimens consist of spheroidal and sub-spheroidal macroids, c. 6 cm in mean diameter, with the asymmetric concentric inner arrangement of *Acervulina inhaerens* crusts intergrown with subordinate thin hapalidialean coralline algae. *Entobia* isp., *Maeandropolydora* isp., *Trypanites* isp., micro-endolithic traces, with rare *Gastrochaenolites* isp., represent the bioerosion traces. Radiocarbon chronology gave an oldest date of c. 4400 cal yr BP for the earliest acervulinid growth. Individual nodules show two growth stages with a long (up to c. 1000 years) and a highly varying growth hiatus between them. No temporal patterns of growth interruption among the dated nine specimens were observed.

The macroid-forming encrusting acervulinids have been growing under low sedimentation rate, low water turbulence, and a maximum range of palaeotemperature changes of c. 4.7 °C at least during the latest Middle to Late Holocene. They outcompeted phototrophic organisms, such as hermatypic corals and coralline algae, for substrate encrustation.

The lack of synchronicity in the individual macroids excludes ecosystem-wide causes of growth interruption, including catastrophic events (large tsunamis). Random biogenic mobilization and burial and temporal occupation of macroid surface by organisms or biofilms are likely responsible of interruptions of macroid growth. Soft-bodied organisms, such as sponges, and biofilms prevented acervulinid growth and boring bivalve settlement on macroid surfaces. Assumptions of environmental factors affecting whole macroid/rhodolith beds need to be supported by a significant number of datings of growth phases and hiatuses in individual nodules.

The environmental conditions of Kikai-jima macroids contradict interpretations of acervulinids as opportunistic foraminifera indicating eutrophic environments and deterioration of trophic conditions in Paleocene–Eocene (PETM) and middle Eocene (MECO) Western Tethyan carbonate factories. Rather, their flourishing is likely due to limited competition for space with phototrophic organisms.

## CRediT authorship contribution statement

**Davide Bassi:** Writing – review & editing, Writing – original draft, Validation, Methodology, Investigation, Funding acquisition, Formal analysis, Data curation, Conceptualization. **Juan Carlos Braga:** Writing

– review & editing, Writing – original draft, Validation, Methodology, Investigation, Formal analysis, Data curation. **Ryuji Asami:** Writing – original draft, Validation, Methodology, Formal analysis, Data curation. **Kazuhsisa Goto:** Writing – original draft, Validation, Investigation. **Sönke Szidat:** Writing – original draft, Methodology, Formal analysis. **Hideko Takayanagi:** Writing – original draft, Methodology, Formal analysis, Data curation. **Yasufumi Iryu:** Writing – review & editing, Writing – original draft, Validation, Investigation, Funding acquisition, Formal analysis.

## Declaration of competing interest

The authors declare that they have no known competing financial interests or personal relationships that could have appeared to influence the work reported in this paper.

## Data availability

No data was used for the research described in the article.

## Acknowledgements

This investigation was financially supported in part by Grants in Aid for Scientific Research, Japan Society for the Promotion of Science (18340163 and 21340152 to YI) and by local research funds (FAR 2018–2022) at the University of Ferrara (DB). This paper is a scientific contribution of the PRIN 2017RX9XXX (Biota resilience to global change: biomimeticization of planktic and benthic calcifiers in the past, present and future). This study was partly financially supported by Frontier Research in Duo (FRID) of Tohoku University and by World Premier International Research Center Initiative (WPI), MEXT, Japan, to YI. DB sincerely acknowledges the International Research Fellow of the Japan Society for the Promotion of Science (JSPS, S21080) at the Institute of Geology and Paleontology, Graduate School of Science, Tohoku University (Sendai, Japan). Sincere thanks are expressed to the Institute of Geology and Paleontology, Graduate School of Environmental Studies, Tohoku University, for inviting DB to Sendai, Japan. The photo in Fig. 2A was provided by K. Arai. Reviews and comments by the Editor and two anonymous reviewers are much appreciated.

## References

- Abram, N.J., Webster, J.M., Davies, P.J., Dullo, W.C., 2001. Biological response of coral reefs to sea surface temperature variation: evidence from the raised Holocene reefs of Kikai-jima (Ryukyu Islands, Japan). *Coral Reefs* 20, 221–234.
- Adey, W.H., Macintyre, I.G., 1973. Crustose coralline algae: a re-evaluation in the geological sciences. *Geol. Soc. Am. Bull.* 84, 883–904.
- Adey, W.H., Townsend, R., Boykins, W., 1982. The crustose coralline algae of the Hawaiian Islands. *Smithson. Contrib. Mar. Sci.* 15, 1–74.
- Aftabuzzaman, Md., Yomogida, K., Suzuki, S., Takayanagi, H., Ishigaki, A., Machida, S., Asahara, Y., Yamamoto, K., Hirano, N., Sano, S.-I., Chiyonobu, S., Bassi, D., Iryu, Y., 2021. Multi-approach characterization of shallow-water carbonates off Minamitorishima and their depositional settings/history. *Island Arc* 30, e12400.
- Aguirre, J., Braga, J.C., 2022. Middle Miocene (Serravallian) rhodoliths and coralline algal debris in carbonate ramps (Betic Cordillera, S Spain). *Front. Earth Sci.* 10, 958148.
- Aguirre, J., Braga, J.C., Martín, J.M., 1993. Algal nodules in the upper Pliocene deposits at the coast of Cádiz (S Spain). In: Barattolo, F., De Castro, P., Parente, M. (Eds.), *Studies on Fossil Benthic Algae*, vol. 1. *Bull. Soc. Paleontol. Ital. Spec.*, pp. 1–7.
- Aguirre, J., Braga, J.C., Martín, J.M., Betzler, C., 2012. Palaeoenvironmental and stratigraphic significance of Pliocene rhodolith beds and coralline algal bioconstructions from the Carboneras Basin (SE Spain). *Geodiversitas* 34, 115–136.
- Aguirre, J., Braga, J.C., Bassi, D., 2017. The role of rhodoliths and rhodolith beds in the rock record and their use in palaeoenvironmental reconstructions. In: Riosmena-Rodríguez, R., Nelson, W., Aguirre, J. (Eds.), *Rhodolith/mäerl beds: a global perspective*. 15. Springer-Verlag, Coast. Res. Libr., pp. 105–138.
- Amado-Filho, G.M., Pereira-Filho, G.H., Bahia, R.G., Abrantes, D.P., Veras, P.C., Matheus, Z., 2012. Occurrence and distribution of rhodolith beds on the Fernando de Noronha Archipelago of Brazil. *Aquat. Bot.* 101, 41–45.
- Amado-Filho, G.M., Bahia, R.G., Pereira-Filho, G.H., Longo, L.L., 2017. South Atlantic rhodolith beds: latitudinal distribution, species composition, structure and ecosystem functions, threats and conservation status. In: Riosmena-Rodríguez, R.,

- Nelson, W., Aguirre, J. (Eds.), Rhodolith/maërl beds: A Global Perspective, 15. Springer-Verlag, Coast. Res. Libr, pp. 299–317.
- Anagnostou, E., John, E.H., Edgar, K.M., Foster, G.L., Ridgwell, A., Inglis, G.N., Pancost, R.D., Lunt, D.J., Pearson, P.N., 2016. Changing atmospheric CO<sub>2</sub> concentration was the primary driver of early Cenozoic climate. *Nature* 533, 380–384.
- Arai, K., Inoue, T., Matsuda, H., Machiyama, H., Sasaki, K., Iryu, Y., Sugihara, K., Fujita, K., Nara, M., 2008. Shallow seismic profiling survey on postglacial fore-reef near the present-day northern limit of coral reef formation in the northwestern Pacific. In: Proc. 11th Int. Coral Reef Symp. Ft. Lauderdale, session no. 2, pp. 9–52.
- Arai, K., Machiyama, H., Chiyonobu, S., Matsuda, H., Sasaki, K., Humblet, M., Iryu, Y., 2014. Subsidence of the Miyako-Sone submarine carbonate platform, east of Miyakojima Island, northwestern Pacific Ocean. *Isl. Arc* 23, 1–15.
- Asami, R., Yoshimura, N., Toriyabe, H., Minei, S., Shinjo, R., Hongo, C., Sakamaki, T., Fujita, K., 2020. High-resolution evidence for middle Holocene East Asian winter and summer monsoon variations: snapshots of fossil coral records. *Geophys. Res. Lett.* 47 e2020GL088509.
- Baarli, B.G., Santos, A., da Silva, C.M., Ledesma-Vázquez, J., Mayoral, E., Cachao, M., Johnson, M.E., 2012. Diverse macrooids and rhodoliths from the upper Pleistocene of Baja California Sur, Mexico. *J. Coast. Res.* 28, 296–305.
- Baceta, J.I., Pujalte, V., Bernaola, G., 2005. Paleocene corallal reefs of the western Pyrenean basin, northern Spain: new evidence supporting an earliest Paleogene recovery of reefal ecosystems. *Palaeogeogr. Palaeoclimatol. Palaeoecol.* 224, 117–143.
- Bassi, D., 1995. Crustose coralline algal pavements from late Eocene – Colli Berici of Northern Italy. *Riv. Ital. Paleontol. Stratigr.* 101, 81–92.
- Bassi, D., 2003. Reassessment of *Solenomeris afonensis* Maslov, 1956 (Foraminifera): formerly considered a coralline red alga. *Rev. Esp. Micropaleontol.* 35, 357–363.
- Bassi, D., Carannante, G., Murru, M., Simone, L., Toscano, F., 2006. Rhodagal/bryomol assemblages in temperate type carbonate, channelised depositional systems: the early Miocene of the Sarcidano area (Sardinia, Italy). In: Pedley, H.M., Carannante, G. (Eds.), Cool-Water Carbonates: Depositional Systems and Palaeoenvironmental Control, 255. Geol. Soc. London, Spec. Publ, pp. 35–52.
- Bassi, D., Carannante, G., Checconi, A., Simone, L., Vigorito, M., 2010. Sedimentological and palaeoecological integrated analysis of a Miocene canalized coralline red algal carbonate margin (Matese Mountains, Central-Southern Apennines, Italy). *Sediment. Geol.* 230, 105–122.
- Bassi, D., Humblet, M., Iryu, Y., 2011. Recent ichnocoenoses in deep water macrooids, Ryukyu Islands, Japan. *Palaios* 26, 232–238.
- Bassi, D., Iryu, Y., Humblet, M., Matsuda, H., Machiyama, H., Sasaki, K., Matsuda, S., Arai, K., Inoue, T., 2012. Recent macrooids on the Kikai-jima shelf, Central Ryukyu Islands, Japan. *Sedimentology* 59, 2024–2041.
- Bassi, D., Iryu, Y., Braga, J.C., Takayanagi, H., Tsuji, T., 2013. Bathymetric distribution of ichnocoenoses from recent subtropical algal nodules off Fraser Island, eastern Australia. *Palaeogeogr. Palaeoclimatol. Palaeoecol.* 369, 58–66.
- Bassi, D., Simone, L., Nebelsick, J.H., 2017. Re-sedimented rhodoliths in channelized depositional systems. In: Riósmaña-Rodríguez, R., Nelson, W., Aguirre, J. (Eds.), Rhodolith/maërl beds: A Global Perspective, 15. Springer-Verlag, Coast. Res. Libr, pp. 139–167.
- Bassi, D., Braga, J.C., Owada, M., Aguirre, J., Lipps, J.H., Takayanagi, H., Iryu, Y., 2020. Boring bivalve traces in modern reef and deeper water macroid and rhodolith beds. *Prog. Earth Planet. Sci.* 7, 41.
- Beckmann, J.P., Bolli, H.M., Kleboth, P., Decima, F.P., 1982. Micropaleontology and biostratigraphy of the Campanian to Paleocene of the Monte Giglio, Bergamo Province, Italy. *Mem. Sci. Geol.* 35, 91–172.
- Berger, A., Loutre, M.F., 1991. Insolation values for the climate of the last 10 millions years. *Quat. Sci. Rev.* 10, 297–317.
- Bosellini, A., Ginsburg, R.N., 1971. Form and internal structure of recent algal nodules (rhodolites) from Bermuda. *J. Geol.* 79, 669–682.
- Bosence, D.W.J., 1991a. Description and classification of rhodoliths (rhodoids, rhodolites). In: Peryt, T.M. (Ed.), Coated Grains. Springer, Berlin, pp. 217–224.
- Bosence, D.W.J., 1991b. Coralline algae: Mineralization, taxonomy, and palaeoecology. In: Riding, R. (Ed.), Calcareous Algae and Stromatolites. Springer-Verlag, Berlin, pp. 98–113.
- Bosence, D.W., Pedley, H.M., 1982. Sedimentology and palaeoecology of a Miocene coralline algal biostrome from the Maltese Islands. *Palaeogeogr. Palaeoclimatol. Palaeoecol.* 38, 9–43.
- Bowman, J.P., 2007. Bioactive compound synthetic capacity and ecological significance of marine bacterial genus *Pseudoalteromonas*. *Mar. Drugs* 5, 220–241.
- Bracchi, V.A., Purkis, S.J., Marchese, F., Nolan, M.K.B., Terraneo, T.I., Vimercati, S., Chimienti, G., Rodriguez, M., Eweida, A., Benzioni, F., 2023. Mesophotic foraminiferal-algal nodules play a role in the Red Sea carbonate budget. *Commun. Earth Environ.* 4, 288.
- Braga, J.C., Martín, J.M., 1988. Neogene coralline-algal growth-forms and their palaeoenvironments in the Almanzora River Valley (Almería, SE Spain). *Palaeogeogr. Palaeoclimatol. Palaeoecol.* 67, 285–303.
- Brandano, M., Tomasetti, L., 2022. MECO and Alpine orogenesis: constraints for facies evolution of the Bartonian nummulitic and *Solenomeris* limestone in the Argentina Valley (Ligurian Alps). *Sedimentology* 69, 24–46.
- Brasileiro, P.S., Braga, J.C., Amado-Filho, G.M., Leal, R.N., Bassi, D., Franco, T., Bastos, A.C., Moura, R.L., 2018. Burial rate determines Holocene rhodolith development on the Brazilian Shelf. *Palaios* 33, 464–477.
- Bromley, R.G., 1994. The palaeoecology of bioerosion. In: Donovan, S.K. (Ed.), The Palaeobiology of Trace Fossils. John Wiley and Sons, Chichester, pp. 134–154.
- Caratelli, M., Archiby, F.M., Fürsch, F., Pignatti, J., 2021. Macroids from mixed siliciclastic-carbonate high-frequency sequences of the Agrio Formation (lower cretaceous), Neuquén Basin: palaeoecological and palaeoenvironmental constraints. *Cretac. Res.* 123, 104778.
- Caron, V., Deschamps, B., Robert-Duarte, A., Bailleul, J., 2023. New quantitative descriptors (shape and macroborings) of biogenic nodules: examples from the Lesser Antilles and New Zealand. *Palaios* 38, 491–505.
- Checconi, A., Bassi, D., Monaco, P., Carannante, G., 2010. Re-deposited rhodoliths in the Middle Miocene hemipelagic deposits of Vitulano (Southern Apennines, Italy): coralline assemblage characterization and related trace fossils. *Sediment. Geol.* 225, 50–66.
- Chuang, K.-Y., Asami, R., Takayanagi, H., Morimoto, M., Abe, O., Nakamori, T., Iryu, Y., 2023. Multidecadal-to-interannual modulations of late Holocene climate variations reconstructed from oxygen isotope ratios of a 237-year-long lived fossil coral in Kikai Island, southwestern Japan. *Quat. Sci. Rev.* 322, 108392.
- Coletti, G., Mariani, L., Garzanti, E., Consani, S., Bosio, G., Vezzoli, G., Hu, X., Basso, D., 2021. Skeletal assemblages and terrigenous input in the Eocene carbonate systems of the Nummulitic Limestone (NW Europe). *Sediment. Geol.* 425, 106005.
- Darga, R., 1993. Notable growth forms of the foraminifera *Gypsina linearis* (Hanzawa, 1945) from the carbonate platform of Eisenrichterstein near Hallthurm, Upper Eocene, Bavaria, northern Calcareous Alps. *Zitteliana* 20, 253–261.
- Douville, H., 1924. Un nouveau genre d'Algues calcaires. *C. r. somm. Séances Soc. géol. Fr.* 4e sér. 24 (16), 169–170.
- Eichenseer, H., Luterbacher, H., 1992. The marine Paleogene of the Tremp region (NE Spain)-depositional sequences, facies history, biostratigraphy and controlling factors. *Facies* 27, 119–151.
- Elliott, G.F., 1964. Tertiary solenoporacean algae and the reproductive structures of the Solenoporaceae. *Palaeontology* 7, 695–702.
- Ferratges, F.A., Zamora, S., Aurell, M., 2021. Unravelling the distribution of decapod crustaceans in the lower Eocene coral reef mounds of NE Spain (Tremp-Graus Basin, southern Pyrenees). *Palaeogeogr. Palaeoclimatol. Palaeoecol.* 575, 110439.
- Figueiredo, M.A.O., Eide, I., Reynier, M., Villas-Boás, A.B., Tâmega, F.T.S., Ferreira, C.G., Nilssen, I., Coutinho, R., Johnsen, S., 2015. The effect of sediment mimicking drill cuttings on deep-water rhodoliths in a flow-through system: experimental work and modelling. *Mar. Pollut. Bull.* 95, 81–88.
- Focke, J.W., Gebelein, C.D., 1978. Marine lithification of reef rock and rhodolites at a fore-reef slope locality (- 50 m) off Bermuda. *Geol. Mijnb.* 57, 163–171.
- Foster, M.S., Amado Filho, G.M., Kamenos, N.A., Riósmaña-Rodríguez, R., Steller, D.L., 2013. Rhodoliths and rhodolith beds. *Smithson. Contrib. Mar. Sci.* 39, 143–155.
- Frantz, B.R., Kashgarian, M., Coale, K.H., Foster, M.S., 2000. Growth rate and potential climate record from a rhodolith using <sup>14</sup>C accelerator mass spectrometry. *Limnol. Oceanogr.* 45, 1773–1777.
- Fujiwara, O., Goto, K., Ando, R., Garrett, E., 2020. Paleotsunami research along the Nankai Trough and Ryukyu Trench subduction zones – current achievements and future challenges. *Earth Sci. Rev.* 210, 103333.
- Garas, K.L., Watanabe, T., Yamazaki, A., 2023. Hydroclimate seasonality from paired coral Sr/Ca and <sup>81</sup>O records of Kikai Island, southern Japan: evidence of East Asian monsoon during mid-to-late Holocene. *Quat. Sci. Rev.* 301, 107926.
- Golubic, S., Radtke, G., 2005. Endolithic fungi in marine ecosystems. *Trends Microbiol.* 13, 229–235.
- Gómez-Lemos, L.A., Diaz-Pulido, G., 2017. Crustose coralline algae and associated microbial biofilms deter seaweed settlement on coral reefs. *Coral Reefs* 36, 453–462.
- Goto, K., 2017. Paleo tsunami researches along the Ryukyu Trench. *J. Geol. Soc. Japan* 123, 843–855 (in Japanese).
- Gottschalk, J., Szidat, S., Michel, E., Mazaud, A., Salazar, G., Battaglia, M., Lippold, J., Jaccard, S.L., 2018. Radiocarbon measurements of small-size foraminiferal samples with the mini carbon dating system (MICADAS) at the University of Bern: implications for paleoclimate reconstructions. *Radiocarbon* 60, 469–491.
- Graham, D.J., Midgley, N.G., 2000. Graphical representation of particle shape using triangular diagrams: an excel spreadsheet method. *Earth Surf. Process. Landf.* 25, 1473–1477.
- Hagn, H., Wellnhofer, P., 1967. Ein erratisches Vorkommen von kalkalpinen Obereozän in Pfaffind bei Wasserburg. *Geol. Bavaria* 57, 205–288.
- Halfar, J., Adey, W.H., Kronz, A., Hetzinger, S., Edinger, E., Fitzhugh, W.W., 2013. Arctic Sea-ice decline archived by multicentury annual-resolution record from crustose coralline algal proxy. *Proc. Natl. Acad. Sci.* 110, 1973736–1973741.
- Hamamoto, K., Reimer, J.D., 2022. Ascidians observed associating epizooically on holothurians in waters in the Kerama Islands, Okinawa, Japan. *Plankton Benthos Res.* 17, 338–342.
- Heaton, T.J., Kohler, P., Butzin, M., Bard, E., Reimer, R.W., Austin, W.E., Ramsey, C.B., Grootes, P.M., Hughen, K.A., Kromer, B., Reimer, P.J., Adkins, J., Burke, A., Cook, M. S., Olsen, J., Skinner, L., 2020. Marine20—the marine radiocarbon age calibration curve (0–55,000 cal BP). *Radiocarbon* 62, 779–820.
- Henehan, M.J., Edgar, K.M., Foster, G.L., Penman, D.E., Pincelli, M.H., Greenop, R., Anagnostou, E., Pearson, P.N., 2020. Revisiting the Middle Eocene Climatic Optimum “carbon cycle conundrum” with new estimates of atmospheric pCO<sub>2</sub> from Boron isotopes. *Paleoceanogr. Paleoclimatol.* 35, e2019PA003713.
- Hirabayashi, S., Yokoyama, Y., Suzuki, A., Miyairi, Y., Aze, T., 2017. Short-term fluctuations in regional radiocarbon reservoir age recorded in coral skeletons from the Ryukyu Islands in the North-Western Pacific. *J. Quat. Sci.* 32, 1–6.
- Hohenegger, J., 1999. Larger foraminifera – Microscopical greenhouse indicating shallow-water tropical and subtropical environment in the present and past. In: Kagoshima Univ. Res. Cent. Pacific Islands, Occas. Pap., 32, pp. 19–45.
- Hori, N., 1983. New terms for coral reef geomorphology. In: Proc. Gen. Meet. Assoc. Jap. Geograph., 24, pp. 76–77 (in Japanese).
- Hottinger, L., 1983. Neritic macroid genesis, an ecological approach. In: Peryt, T.M. (Ed.), Coated Grains. Springer-Verlag, Berlin, pp. 38–55.

- Hottinger, L., Levinson, G., 1978. Cementation of reefs in the Gulf of Elat (Red Sea) by *Acervulinid* Foraminifera. In: 10th Int. Congr. Sedim., Jerusalem, Abstr. 315.
- Iryu, Y., 1984. Discovery of recent deep water rhodoliths from the Ryukyu Islands, southwestern Japan, and its significance. In: Prompt Rep. Compreh. Sci. Surv. Ryukyu Archipelago, vol. 1. Kagoshima Univ, pp. 47–55 (in Japanese with English abstract).
- Iryu, Y., 1985. Study on the recent rhodoliths around the Ryukyu Islands. In: Prompt Rep. Compreh. Sci. Surv. Ryukyu Archipelago, vol. 2. Kagoshima Univ, pp. 123–133 (in Japanese with English abstract).
- Iryu, Y., Nakamori, T., Matsuda, S., Abe, O., 1995. Distribution of marine organisms and its geological significance in the modern reef complex of the Ryukyu Islands. *Sediment. Geol.* 99, 243–258.
- Iryu, Y., Nakamori, T., Yamada, T., 1998. Pleistocene reef complex deposits in the Central Ryukyus, southwestern Japan. In: Camoin, G., Davies, P.J. (Eds.), *Reefs and Carbonate Platforms in the Pacific and Indian Oceans*. Spec. Publ. I.A.S, vol. 25. Blackwell Science, Oxford, pp. 197–213.
- Iryu, Y., Matsuda, H., Machiyama, H., Piller, W.E., Quinn, T.M., Mutti, M., 2006. An introductory perspective on the COREF Project. *Isl. Arc* 15, 393–406.
- Johnson, M.E., da Silva, C.M., Santos, A., Gudveig Baarli, B., Cachão, M., Mayoral, E.J., Cristina Rebelo, A.C., Ledesma-Vázquez, J., 2011. Rhodolith transport and immobilization on a volcanically active rocky shore: Middle Miocene at Cabeço das Laranjas on Ilhéu de Cima (Madeira Archipelago, Portugal). *Palaeogeogr. Palaeoclimatol. Palaeoecol.* 300, 113–127.
- Johnson, M.E., Ledesma-Vázquez, J., Ramalho, R.S., da Silva, C.M., Santos, A., Baarli, G., Mayoral, E.J., Cachão, M., 2017. Taphonomic range and sedimentary dynamics of modern and fossil rhodolith beds: Macaronesian realm (North Atlantic Ocean). In: Riosmena-Rodríguez, R., Nelson, W., Aguirre, J. (Eds.), *Rhodolith/maërl Beds: A Global Perspective*, 15. Springer-Verlag, Coast. Res. Libr, pp. 221–261.
- Juillet-Leclerc, A., Schmidt, G., 2001. A calibration of the oxygen isotope paleothermometer of coral aragonite from *Porites*. *Geophys. Res. Lett.* 28, 4135–4138.
- Kajita, H., Yamazaki, A., Watanabe, T., Wu, C.-C., Shen, C.-C., Watanabe, T., 2017. Holocene Sea surface temperature variations recorded in corals from Kikai Island, Japan. *Geochem. J.* 51, e9–e14.
- Kamenos, N.A., Heidi, L.B., Darrenougue, N., 2017. Coralline algae as recorders of past climatic and environmental conditions. In: Riosmena-Rodríguez, R., Nelson, W., Aguirre, J. (Eds.), *Rhodolith/maërl Beds: A Global Perspective*. Springer, Berlin Heidelberg, pp. 27–53.
- Karabiyikoglu, M., Tuzcu, S., Ciner, A., Deynoux, M., Örcen, S., Hakyemez, A., 2005. Facies and environmental setting of the Miocene coral reefs in the late-orogenic fill of the Antalya Basin, western Taurides, Turkey: implications for tectonic control and sea-level changes. *Sediment. Geol.* 173, 345–371.
- Kato, Y., 1993. Geological structure and topography of the Amami Plateau. *Rep. Hydrogr. Res.* 29 (1993), 51–63 (in Japanese with English abstract).
- Kawahata, H., Fujita, K., Iguchi, A., Inoue, M., Iwasaki, S., Kuwayanagi, A., Maeda, A., Manaka, T., Moriya, K., Takagi, H., Toyofuku, T., Yoshimura, T., Suzuki, A., 2019. Perspective on the response of marine calcifiers to global warming and ocean acidification—Behaviour of corals and foraminifera in a high CO<sub>2</sub> world “hot house”. *Prog. Earth Planet. Sci.* 6, 5.
- Kawakubo, Y., Alibert, C., Yokoyama, Y., 2017. A reconstruction of subtropical western North Pacific SST variability back to 1578, based on a *Porites* coral Sr/Ca record from the Northern Ryukyus, Japan. *Paleoceanography* 32, 1352–1370.
- Kawana, T., 1989. Quaternary crustal movement in the Ryukyu Islands. *Earth Monthly* 11, 618–630 (in Japanese, original title translated).
- Kiyama, O., Yamada, T., Nakamori, T., Iryu, Y., 2000. Early Holocene coral δ<sup>18</sup>O-based sea surface temperature. *Quat. Res.* 39, 69–80 (in Japanese).
- Krautwig, D.W.H., Hottinger, L., Zankl, H., 1998. Lamellar-perforate, arborescent and coloured foraminifera *Miniacina*, *Homotrema*, and *Sporadotrema*. *Facies* 38, 89–102.
- Krug, P.J., 2006. Defence of benthic invertebrates against surface colonization by larvae: a chemical arms race. In: Fusetani, N., Clare, A.S. (Eds.), *Antifouling compounds. Progr. Mol. Subcel. Biol. Marine Molecular Biotechnology*, 42. Springer-Verlag, Berlin, pp. 1–53.
- Lavenère-Wanderley, A.A., Asp, N.E., Thompson, F.L., Siegle, E., 2021. Rhodolith mobility potential from seasonal and extreme waves. *Cont. Shelf Res.* 228, 104527.
- Leutenegger, S., 1984. Symbiosis in benthic foraminifera; specificity and host adaptations. *J. Foraminif. Res.* 14, 16–35.
- Lewis, B., Lough, J.M., Nash, M.C., Diaz-Pulido, G., 2017. Presence of skeletal banding in a reef-building tropical crustose coralline alga. *PLoS One* 12, e0185124.
- Li, Q., Li, G., Chen, M.-T., Xu, J., Liu, S., Chen, M., 2020. New insights into Kuroshio current evolution since the last deglaciation based on paired organic paleothermometers from the middle Okinawa Trough. *Paleoceanogr. Paleoclimatol.* 35, e2020PA004140.
- Littler, D.S., Littler, M.M., 2003. South Pacific Reef Plants. A divers' Guide to the Plant Life of South Pacific Coral Reefs. Offshore Graphics, Washington, p. 331.
- Littler, M.M., Littler, D.S., Hanisak, M.D., 1991. Deep-water rhodolith distribution, productivity, and growth history at sites of formation and subsequent degradation. *J. Exp. Mar. Biol. Ecol.* 150, 163–182.
- Lund, M., Davies, P.J., Braga, J.C., 2000. Coralline algal nodules off Fraser Island, eastern Australia. *Facies* 42, 25–34.
- Maida, M., Sammarco, P.W., Coll, J.C., 1995. Effects of soft corals on scleractinian coral recruitment. I: directional allelopathy and inhibition of settlement. *Mar. Ecol. Prog. Ser.* 121, 191–202.
- Marrack, E.C., 1999. The relationship between water motion and living rhodolith beds in the southwestern gulf of California, Mexico. *Palaios* 14, 159–171.
- Martín-Martín, M., Guerrera, F., Tosquella, J., Tramontana, M., 2021. Middle Eocene carbonate platforms of the westernmost Tethys. *Sediment. Geol.* 415, 105861.
- Matsuda, S., Iryu, Y., 2011. Rhodoliths from deep fore-reef to shelf areas around Okinawa-jima, Ryukyu Islands, Japan. *Mar. Geol.* 282, 215–230.
- Matsuda, S., Nohara, M., 1994. Radiocarbon ages of rhodoliths on the deep forereef to insular shelves around Okinawa-jima, Ryukyu Islands. *Bull. Coll. Edu. Univ. Ryukyus* 44, 185–193 (in Japanese with English abstract).
- Matsuda, H., Arai, K., Inoue, T., Machiyama, H., Sasaki, K., Iryu, Y., Fujita, K., Humbert, M., Sugihara, K., Nara, M., 2010. Rhodolith-bearing gravelly carbonate sediments on the shelf off Kikai Island, Kagoshima Prefecture. *J. Sediment. Soc. Japan* 69, 62.
- Matsuda, H., Arai, K., Machiyama, H., Iryu, Y., Tsuji, Y., 2011. Submerged reefal deposits near a present-day northern limit of coral reef formation in the northern Ryukyu Island Arc, northwestern Pacific Ocean. *Isl. Arc* 20, 411–425.
- McInerney, F.A., Wing, S.L., 2011. The Paleocene–Eocene thermal maximum: a perturbation of carbon cycle, climate, and biosphere with implications for the future. *Annu. Rev. Earth Planet. Sci.* 39, 489–516.
- McMaster, R.L., Conover, J.T., 1966. Recent algal stromatolites from Canary Islands. *J. Geol.* 74, 647–652.
- Ministry of the Environment and Japanese Coral Reef Society, 2004. *Coral Reefs of Japan*. Ministry of Environment, Tokyo, p. 286. [https://www.jcrs.jp/old/english/publications/coralreefsjapan\\_top.htm](https://www.jcrs.jp/old/english/publications/coralreefsjapan_top.htm).
- Minnery, G.A., 1990. Crustose coralline algae from the Flower Garden Banks, northwestern Gulf of Mexico: controls on distribution and growth morphology. *J. Sediment. Petrol.* 60, 992–1007.
- Morimoto, M., Kayanne, H., Abe, O., McCulloch, M., 2007. Intensified mid-Holocene Asian monsoon recorded in corals from Kikai Island, subtropical northwestern Pacific. *Quat. Res.* 67, 204–214.
- Moussavian, E., Höfling, R., 1993. Taxonomische Position und Palökologie von *Solenomeris Douvilléi*, 1924 und ihre Beziehung zu *Acervulina Schultze*, 1854 und *Gypsina Carter*, 1877 (Acervulinidae, Foraminiferida). *Zitteliana* 20, 263–276.
- Murru, M., Bassi, D., Simone, L., 2015. Displaced/re-worked rhodolith deposits infilling parts of a complex Miocene multistorey submarine channel: a case history from the Sassari area (Sardinia, Italy). *Sediment. Geol.* 326, 94–108.
- Nakamori, T., Iryu, Y., Yamada, T., 1995. Development of coral reefs of the Ryukyu Islands (Southwest Japan, East China Sea) during Pleistocene Sea-level change. *Sediment. Geol.* 99, 215–231.
- Nakamura, H., Ichikawa, H., Nishina, A., 2007. Numerical study of the dynamics of the Ryukyu current system. *J. Geophys. Res.* 112, C04016.
- Nakata, T., Takahashi, T., Koba, M., 1978. Holocene-emerged coral reefs and sea-level changes in the Ryukyu Islands. *Geogr. Rev. Japan* 51, 87–108 (in Japanese with English abstract).
- Nebelsick, J.H., Rasser, M., Bassi, D., 2005. Facies dynamics in Eocene to Oligocene Circumalpine carbonates. *Facies* 51, 197–216.
- Nitsch, F., Nebelsick, J.H., Bassi, D., 2015. Constructional and destructional patterns – Void classification of rhodoliths from Giglio Island, Italy. *Palaios* 30, 680–691.
- O'Connell, L.G., James, N.P., Harvey, A.S., Luick, J., Bone, Y., Shepherd, S.A., 2021. Reevaluation of the inferred relationship between living rhodolith morphologies, their movement, and water energy: implications for interpreting paleoceanographic conditions. *Palaios* 35, 543–556.
- Ota, Y., Machida, H., Horii, N., Konishi, K., Omura, A., 1978. Holocene raised coral reefs of Kikai-jima (Ryukyu Islands) – an approach to Holocene Sea level study. *Geograph. Rev. Japan* 51 (2), 109–130 (in Japanese with English abstract).
- Ota, Y., Machida, K., Omura, A., Nozawa, K., 2000. Holocene Sea level and tectonic history related to the formation of coral terraces at Ikai Island, Northern Ryukyu Island. *Quat. Res.* 29, 81–95 (in Japanese with English abstract).
- Pálfalvi, S., 2004. Palaeoenvironments on a Middle Eocene carbonate ramp in the Vértes Mountains, Hungary. *Hantkeniana* 4, 63–81.
- Palmieri, V., Jell, J.S., 1985. Recruitment of encrusting Foraminifers on Heron reef, Great Barrier Reef (Queensland, Australia). In: Proc. 5th Int. Coral Reef Congr. Tahiti, pp. 221–226.
- Perrin, C., 1987. *Solenomeris*: un Foraminifère Acervulinidae constructeur de récifs. *Rev. Micropaleontol.* 30, 197–206.
- Perrin, C., 1992. Signification écologique des foraminifères acervulinidés et leur rôle dans la formation de faciès récifaux et organogènes depuis le Paléocène. *Geobios* 25, 725–751.
- Perrin, C., 1994. Morphology of encrusting and free living acervulinid foraminifera: *Acervulina*, *Gypsina* and *Solenomeris*. *Palaeontology* 37, 425–458.
- Perrin, C., 2009. *Solenomeris*: from biomineralization patterns to diagenesis. *Facies* 55, 501–522.
- Perry, C.T., Hepburn, L.J., 2008. Syn-depositional alteration of coral reef framework through bioerosion, encrustation and cementation: taphonomic signatures of reef accretion and reef depositional events. *Earth Sci. Rev.* 86, 106–144.
- Plaziat, J.-C., Perrin, C., 1992. Multikilometer-sized reefs built by foraminifera (*Solenomeris*) from the early Eocene of the Pyrenean domain (S. France, N. Spain): palaeoecologic relations with coral reefs. *Palaeogeogr. Palaeoclimatol. Palaeoecol.* 96, 195–231.
- Poisson, A., Poignant, A.F., 1975. La formation de Karabiyir, base de la transgression miocène dans la région de Korkuteli (Département d'Antalya-Turquie). *Lithothamnium pseudoramossissimum*, nouvelle espèce d'Algue Rouge de la formation de Karabiyir. *Bull. Min. Res. Expl. Inst. Turkey* 82, 97–71.
- Prager, E.J., Ginsburg, R.N., 1989. Carbonate nodule growth on Florida's outer shelf and its implications for fossil interpretations. *Palaios* 4, 310–317.
- Puga-Bernabéu, A., Aguirre, J., 2017. Contrasting storm- versus tsunami-related shell beds in shallow-water ramps. *Palaeogeogr. Palaeoclimatol. Palaeoecol.* 471, 1–14.
- Rasser, M., 1994. Facies and palaeoecology of rhodoliths and acervulinid macrooids in the Eocene of the Krappfeld (Austria). *Beitr. Palaeontol.* 19, 191–217.

- Reiss, Z., Hottinger, L., 1984. The Gulf of Aqaba: Ecological Micropaleontology. Ecological Studies 50. Springer-Verlag, Berlin, p. 354 pp.
- Robless-Salcedo, R., Rivas, G., Vicedo, V., Caus, E., 2013. Paleoenvironmental distribution of larger foraminifera in Upper cretaceous siliciclastic-carbonate deposits (Arén Sandstone Formation, South Pyrenees, northeastern Spain). *Palaios* 28, 637–648.
- Sagawa, N., Nakamori, T., Iryu, Y., 2001. Pleistocene reef development in the Southwest Ryukyu Islands, Japan. *Palaeogeogr. Palaeoclimatol. Palaeoecol.* 175, 303–323.
- Sánchez-Suárez, J., Díaz, L., Junca, H., García-Bonilla, E., Villamil, L., 2022. Microbiome composition of the marine sponge *Cliona varians* at the neotropical southern Caribbean Sea displays a predominant core of Rhizobiales and Nitrosopumilaceae. *J. Appl. Microbiol.* 133, 2027–2038.
- Scheibner, C., Rasser, M.W., Mutti, M., 2007. The Campo section (Pyrenees, Spain) revisited: implications for changing benthic carbonate assemblages across the Paleocene–Eocene boundary. *Palaeogeogr. Palaeoclimatol. Palaeoecol.* 248, 145–168.
- Schlagintweit, F., Sanders, D., Studeny, M., 2018. The nepionic stage of *Solenomeris* Douvillé, 1924 (Acervulinidae, Foraminifera): new observations from the uppermost Maastrichtian–early Danian of Austria (Kambühel Formation, Northern Calcareous Alps). *Facies* 64, 27.
- Schönberg, C.H.L., Gleason, F.H., Meyer, N., Wissak, M., 2019. Close encounters in the substrate: when macroborers meet microborers. *Facies* 65, 22.
- Schultze, M.J.S., 1854. Über den Organismus der Polythalamien (Foraminiferen), nebst Bemerkungen über die Rhizopoden im allgemeinen. Ingemann, Leipzig, pp. 1–68.
- Shimazaki, K., Nakata, T., 1980. Time-predictable recurrence model for large earthquakes. *Geophys. Res. Lett.* 7, 279–282.
- Sinninger, F., Harii, S., Humbert, M., Nakamura, Y., Ohba, H., Prasetia, R., 2019. Ryukyu Islands, Japan. In: Loya, Y., Puglise, K., Bridge, T. (Eds.), Mesophotic Coral Ecosystems. Coral Reefs of the World, vol. 12. Springer, pp. 231–247.
- Sletten, H.R., Andrus, C.F.T., Guzmán, H.M., Halfar, J., 2017. Re-evaluation of using rhodolith growth patterns for paleoenvironmental reconstruction: an example from the Gulf of Panama. *Palaeogeogr. Palaeoclimatol. Palaeoecol.* 465, 264–277.
- Smith, A.M., Cooper, J.A.G., 2004. Tropical rhodoliths with multiple internal abrasion surfaces: Diani Reef, southern Kenya. *J. Coast. Res.* 21, 74–78.
- Steller, D.L., Foster, M.S., 1995. Environmental factors influencing distribution and morphology of rhodoliths in Bahia Concepcion, B.C.S. Mexico. *J. Exp. Mar. Biol. Ecol.* 194, 201–212.
- Steller, D.L., Riosmena-Rodríguez, R., Foster, M.S., 2009. Living rhodolith ecosystems in the Gulf of California. In: Johnson, J.M., Ledesma-Vázquez, J. (Eds.), Atlas of Coastal Ecosystems in the Gulf of California: Past and Present. University of Arizona Press, Tucson, pp. 72–82.
- Sugihara, K., Nakamori, T., Iryu, Y., Sasaki, K., Blanchon, P., 2003. Holocene Sea-level change and tectonic uplift deduced from raised reef terraces, Kikai-jima, Ryukyu Islands, Japan. *Sediment. Geol.* 159, 5–25.
- Suzuki, Y., Takabayashi, T., Kawaguchi, T., Matsunaga, K., 1998. Isolation of an allelopathic substance from the crustose coralline algae, *Lithophyllum* spp., and its effects on the brown alga, *Laminaria religiosa* Miyabe (Phaeophyta). *J. Exp. Mar. Biol. Ecol.* 225, 69–77.
- Takeyasu, K., Uchiyama, Y., Mitarai, S., 2023. Quantifying connectivity between mesophotic and shallow coral larvae in Okinawa Island, Japan: a quadruple nested high-resolution modelling study. *Front. Mar. Sci.* 10, 1174940.
- Tâmega, F.T.S., Bassi, D., Figueiredo, M.A.O., Cherkinsky, A., 2014. Deep-water rhodolith bed from central Brazilian continental shelf, Campos Basin: coralline algal and faunal taxonomic composition. *Galaxea* 16 (1), 21–31.
- Tâmega, F.T., Spotorno-Oliveira, P., Dentzen-Dias, P., Buchmann, F.S., Vieira, L.M., Macario, K., Nash, M., Guimarães, R.B., Francischini, H., Bassi, D., 2019. Palaeoenvironmental dynamics of Holocene shoreface bryoliths from the southern coast of Brazil. *The Holocene* 29, 662–675.
- Taylor, P.D., Wilson, M.A., 2003. Palaeoecology and evolution of marine hard substrate communities. *Earth Sci. Rev.* 62, 1–103.
- Taylor, M.W., Radax, R., Steger, D., Wagner, M., 2007. Sponge-associated microorganisms: evolution, ecology, and biotechnological potential. *Microbiol. Mol. Biol. Rev.* 71, 295–347.
- Tomás, S., Frijia, G., Bömelburg, E., Zamagni, J., Perrin, C., Mutti, M., 2016. Evidence for seagrass meadows and their response to paleoenvironmental changes in the early Eocene (Jafnayn Formation, Wadi Bani Khalid, N Oman). *Sediment. Geol.* 341, 189–202.
- Tsuji, Y., 1993. Tide influenced high energy environments and rhodolith-associated carbonate deposition on the outer shelf and slope off Miyako Islands, southern Ryukyu Island Arc, Japan. *Mar. Geol.* 113, 255–271.
- Ujiie, H., Nishimura, Y., 1992. Transect of the central and southern Ryukyu Island Arcs. In: 29th IGC Field Trip Guide Book, vol. 5. Metamorphic Belts and Related plutonisms In the Japanese Islands. *Geol. Surv. Japan*, pp. 337–361.
- Vale, N.F.L., Amado-Filho, G.M., Braga, J.C., Brasileiro, P.S., Karez, C.S., Moraes, F.C., Bahia, R.G., Bastos, A.C., Moura, R.L., 2018. Structure and composition of rhodoliths from the Amazon River mouth, Brazil. *J. S. Am. Earth Sci.* 84, 149–159.
- Vale, N.F.L., Braga, J.C., Bastos, A.C., Moraes, F.C., Karez, C.S., Bahia, R.G., Leão, L.A., Pereira, R.C., Amado-Filho, G.M., Salgado, L.T., 2022. Structure and composition of rhodolith beds from the Sergipe-Alagoas Basin (NE Brazil, Southwestern Atlantic). *Diversity* 14, 282.
- van der Heijden, L.H., Kamenos, N.A., 2015. Reviews and syntheses: calculating the global contribution of coralline algae to total carbon burial. *Biogeosciences* 12, 6429–6441.
- Varrone, D., D'Atri, A., 2007. Acervulinid macroid and rhodolith facies in the Eocene Nummulitic Limestone of the Dauphinois Domain (Maritime Alps, Liguria, Italy). *Swiss J. Geosci.* 100, 503–515.
- Veras, P.C., Pierozzi Jr., I., Lino, J.B., Amado-Filho, G.M., De Senna, A.R., Santos, C.S.G., de Moura, R.L., Passos, F.D., Giglio, V.J., Pereira-Filho, G.H., 2020. Drivers of biodiversity associated with rhodolith beds from euphotic and mesophotic zones: insights for management and conservation. *Perspect. Ecol. Conserv.* 18, 37–43.
- Vogel, K., Gektidis, M., Golubic, S., Kiene, W.E., Radtke, G., 2000. Experimental studies on microbial bioerosion at Lee Stocking Island, Bahamas and one tree Island, Great Barrier Reef, Australia: implications for paleoecological reconstructions. *Lethaia* 33, 190–204.
- Walker, S.E., Parsons-Hubbard, K., Richardson-White, S., Brett, C., Powell, E., 2011. Alpha and beta diversity of encrusting foraminifera that recruit to long-term experiments along a carbonate platform-to-slope gradient: paleoecological and paleoenvironmental implications. *Palaeogeogr. Palaeoclimatol. Palaeoecol.* 312, 325–349.
- Wan, S., Xiang, R., Steinke, S., Du, Y., Yang, Y., Wang, S., Wang, H., 2023. Impact of the Western Pacific warm pool and Kuroshio dynamics in the Okinawa Trough during the Holocene. *Glob. Planet. Change* 224, 104116.
- Watanabe, N., Arai, K., Otsubo, M., Toda, M., Tominaga, A., Chiyonobu, S., Sato, T., Ikeda, T., Takahashi, A., Ota, H., Iryu, Y., 2023. Geological history of the land area between Okinawa Jima and Miyako Jima of the Ryukyu Islands, Japan, and its phylogeographical significance for the terrestrial organisms of these and adjacent islands. *Prog. Earth Plan. Sci.* 10, 40.
- Webster, N.S., Taylor, M.W., 2012. Marine sponges and their microbial symbionts: love and other relationships. *Environ. Microbiol.* 14, 335–346.
- Webster, J.M., Davies, P.J., Konishi, K., 1998. Model of fringing reef development in response to progressive sea level fall over the last 7000 years – (Kikai-jima, Ryukyu Islands, Japan). *Coral Reefs* 17, 289–308.
- Whalan, S., Webster, N., 2014. Sponge larval settlement cues: the role of microbial biofilms in a warming ocean. *Sci. Rep.* 4, 4072.
- Wiedl, T., Harzhauser, M., Piller, W.E., 2012. Facies and synsedimentary tectonics on a Badenian carbonate platform in the southern Vienna Basin (Austria, Central Paratethys). *Facies* 58, 523–548.
- Williams, S., Halfar, J., Zack, T., Hetzinger, S., Blicher, M., Juul-Pedersen, T., 2019. Reprint of comparison of climate signals obtained from encrusting and free-living rhodolith coralline algae. *Chem. Geol.* 526, 175–185.
- Woelkerling, W.J., Irvine, L.M., Harvey, A., 1993. Growth-forms in non-geniculate coralline red algae (Corallinales, Rhodophyta). *Aust. Syst. Bot.* 6, 277–293.
- Yoneda, M., Uno, H., Shibata, Y., Suzuki, R., Kumamoto, Y., Yoshida, K., Sasaki, T., Suzuki, A., Kawahata, H., 2007. Radiocarbon marine reservoir ages in the western Pacific estimated by pre-bomb molluscan shells. *Nucl. Instrum. Methods Phys. Res. Sect. B* 259, 432–437.